(NASA-CR-170851) THE SSME HPFTP INTERSTAGE SEALS: ANALYSIS AND EXPERIMENTS FOR LEAKAGE AND REACTION-FORCE COEFFICIENTS Supplementary Progress Report (Texas A&M Univ.) 60 p HC A04/MF A01 CSCL 11A G3/37

N83-34324

Unclas 36078

SSME HPFTP INTERSTAGE SEALS: ANALYSIS AND EXPERIMENTS FOR LEAKAGE AND REACTION-FORCE COEFFICIENTS

PROGRESS REPORT

NASA CONTRACT NAS8-33716

Prepared by

Dara W. Childs, Ph.D., P.E.

Professor of Mechanical Engineering

TURBOMACHINERY LABORATORIES REPORT
SEAL-2-83

July 15, 1983

Turbomachinery Laboratories
Mechanical Engineering Department
Texas A&M University
College Station, Texas 77843

SSME HPFTP INTERSTAGE SEALS: ANALYSIS AND EXPERIMENTS FOR LEAKAGE AND REACTION-FORCE COEFFICIENTS

SUPPLEMENTARY
PROGRESS REPORT

NASA CONTRACT NAS8-33716

Prepared by

Dara W. Childs, Ph.D., P.E.
Professor of Mechanical Engineering

Turbomachinery Laboratories
Mechanical Engineering Department
Texas A&M University
College Station, Texas 77843

TURBOMACHINERY LABORATORIES REPORT
SEAL-2-83

July 15, 1983

SUPPLEMENTARY PROGRESS REPORT - CONTRACT NAS8-33716

Table of Contents

ABSTRACT

An improved theory for the prediction of the rotordynamic coefficients of turbulent annular seals has been developed since the original, 15 February 1983, report [1] on this project. This supplentary report compares predictions from the new theory to the experimental results of [1] and also introduces a new approach for the direct calculation of empirical turbulent coefficients from test data.

An improved short-seal solution is shown to do a better job of calculating effective stiffness and damping coefficients than either the original short-seal solution or a finite-length solution. However, the original short-seal solution does a <u>much</u> better job of predicting equivalent added-mass coefficient.

List of Figures

List of Tables

INTRODUCTION

In the original report [1] on this contract, experimental results were compared to a "short-seal" theoretical model [2] which employed Colebrook's friction-factor formula [3] for predicting turbulent friction-factors. Since reference [1] was completed, an improved finite-length solution procedure [4]* has been developed, and the data have been reanalyzed to directly calculate the Yamada-Hirs [5,6] empirical coefficents. This supplementary report provides a comparison between the experimental data of [1] and the new theory of [4] with empirical friction factor-coefficients which have been directly obtained from the data.

*The analysis is included as Appendix A.

IDENTIFICATION OF EMPIRICAL TURBULENCE COEFFICIENTS FROM TEST DATA

The finite-length-solution development [4] is provided in Appendix A. The leakage formula provided Eq. (15) of this reference is:

$$\Delta P = \left\{ \frac{(1 + \xi)}{(1 + q)^2} + \frac{[2\,\sigma - 2\,\sigma\,\beta\,(1+mo)\,q^2 + 4q]}{(1 - q^2)^2} \right\} \frac{\rho\,\overline{V}^2}{2} \qquad (1)$$

Where

ρ: Fluid density.

ξ = Entry loss coefficient.

$q = \dfrac{Co - C_1}{Co + C_1}$ = Taper parameter.

Co, C_1: Seal entrance and exit clearances, respectively.

$\sigma = \lambda\, L / \overline{C}$

$\lambda = no\, R_{ao}^{mo} \left(1 + \dfrac{1}{4b^2}\right)^{\frac{1+mo}{2}}$: Wall friction factor.

$R_{ao} = 2\, \overline{V}\, \overline{C} / \nu$: Centered-position Reynolds number.

$\overline{C} = (Co + C_1) / 2$: Average seal clearance.

L: Seal length.

γ = Fluid Kinematic viscosity.

$b = \overline{V}/RW$

$\overline{V} = Q/\, 2\pi\, R\, \overline{C}$: Average axial fluid velocity.

Q = Volumetric flow rate.

R = Seal radius.

ω = Shaft angular velocity.

$\beta = 1 / (1 + 4b^2)$

mo, no: Empirical coefficients for the friction-factor definition.

The data for each dynamic seal test includes the inlet and exit chamber pressures and five pressure measurements within the seal. Two of the pressure measurements within the seal are immediately interior to the inlet and exit. The volumetric flowrate and inlet and exit temperatures are also measured. Our objective is to take this data and determine the entry-loss coefficient ξ and the empirical friction-factor coefficients mo, no.

For the ith test case, the total entry-loss factor $(1 + \xi i)$ is readily calculated from the inlet pressure drop relationship

$$\Delta P_{oi} = \frac{(1 + \xi i)}{(1 + q)^2} \cdot \frac{\rho \overline{V} i^2}{2} \tag{2}$$

Eq. (2) was solved directly for $(1 + \xi i)$ for each test case.

The calculations of mo, no for a given test case is relatively straightforward provided λ can be determined from experimental data, since

$$\lambda \left(1 + \frac{1}{4b^2}\right)^{-\frac{1}{2}} = no \left[R_{ao} \left(1 + \frac{1}{4b^2}\right)^{\frac{1}{2}}\right]^{mo} \tag{3}$$

$$\ln \left[\lambda\left(1 + \frac{1}{4b^2}\right)^{-\frac{1}{2}}\right] = \ln (no) + mo \ln \left[R_{ao} \left(1 + \frac{1}{4b^2}\right)\right]^{\frac{1}{2}}$$

Eq. (3) is linear in the parameters ln (no) and mo. Hence, a least-square curve fit of all cases for a given housing-rotor combination will yield the desired data.

The determination of λ from a given data set, i.e., a given rotor-housing combination, represents the principal complication in executing this procedure. The pressure drop within the seal, ΔP_f, is defined as the difference between pressure measurements immediately interior to the inlet and exit of the seal. for case i, Eq. (1) can be expressed:

$$\Delta P_{fi} = \frac{(G_i + 4q)}{(1 - q^2)^2} \cdot \frac{\rho \overline{V}_i^2}{2} \tag{4}$$

Where

$$G_i = 2\, \sigma_i\, [1 - \beta\, (1+mo)\, q^2]$$

The quantity G_i may be readily determined from the experimental data. Hence, one can solve for λ_i as

$$\lambda_i = \overline{C}\, G_i / \, 2L'\, [1 - \beta\, (1+mo)\, q^2] \qquad (5)$$

where L' is the distance between the inlet and exit pressure tops. Direct solution of λ_i from tnis equation is complicated, because mo on the right-hand side is unknown. This difficulty is resolved by an iterative procedure wherein an initial value for mo is guessed, which permits an initial calculation of the λ_i's for all cases in a data set. After the least-square solution yields an estimate for $\overline{mo}$, $\overline{no}$, the procedure is repeated using the updated estimate, $\overline{mo}$. Convergence is rapid since the product $\beta\, (1 + mo)\, q^2$ of Eq. (5) is generally much smaller than unity.

Application of the above procedures yielded the results of Table 1.

Case	Housing	Rotor	no	mo
1	1	1	0.20163	-.2796
2	1	2	0.07106	-.19691
3	1	4	0.00213	.15089
4	1	5	0.00985	.00980
5	2	1	0.07822	-.1182
6	2	4	0.03831	-.0162
7	2	5	0.04330	-.0405
8	3	1	0.02300	-.0377
9	3	4	0.00394	.1448
10	3	5	0.00513	.1118

Table 1. Empirical coefficients for the forced seal data of reference [1] as determined from test data.

Of these ten cases, only the first two have the same directionally-homogeneous surface-roughness treatment for both the rotor and housing. In the remaining cases, a circumferentially-grooved surface roughness treatment was inscribed in either the rotor, the stator, or both rotor and stator. Complete dimensions and surface-roughness measurements for the rotors and stators are provided in reference [1]. For comparative purposes, Yamada's test results for smooth rotor and stators were $n_o = 0.079$; $m_o = -0.25$.

FORCE COEFFICIENT CALCULATION AND COMPARISON

The "finite-length" solution procedure of reference [4] can be run in either a finite-length mode or in an improved short-seal mode. The data of Table 1 were used with the (improved) short-seal and finite-length options of reference [4] to calculate radial and tangential force components for comparison to the tapered-seal test data of reference [1]. Figures 1 through 10 illustrate the results for the finite-length solution, while figures 11 through 20 illustrate the results for the improved short-seal solutions.

The data from these figures were used to calculate effective stiffness, damping, and added-mass coefficients. The results for the finite-length and improved short-seal solution options are provided in tables 2 and 3 respectively. The equivalent comparison between the original short seal theory and experimental results are provided in tables 4 and 5.

A review of the results for all data sets shows no clear superiority for any procedure. As expected, the finite-length solution consistently predicts smaller values for the seal coefficients than either of the short-seal solutions.

As noted earlier, the analyses only strictly apply to the first two data sets for which the same directionally-homogeneous surface roughness holds for both the stator and rotor. To compare the solution approaches for these data sets, the following least-square error calculations were made:

$$EK = \sum_{i=1}^{n} [1 - (KEX/KTH)_i^2] \qquad \text{(Stiffness)}$$

$$EC = \sum_{i=1}^{n} [1 - (CEX/CTH)_i^2] \qquad \text{(Damping)}$$

$$EM = \sum_{i=1}^{n} [1 - (MEX/MTH)_i^2] \qquad \text{(Mass)}$$

where KEX and KTH are the measured and theoretical equivalent direct stiffness respectively, etc.

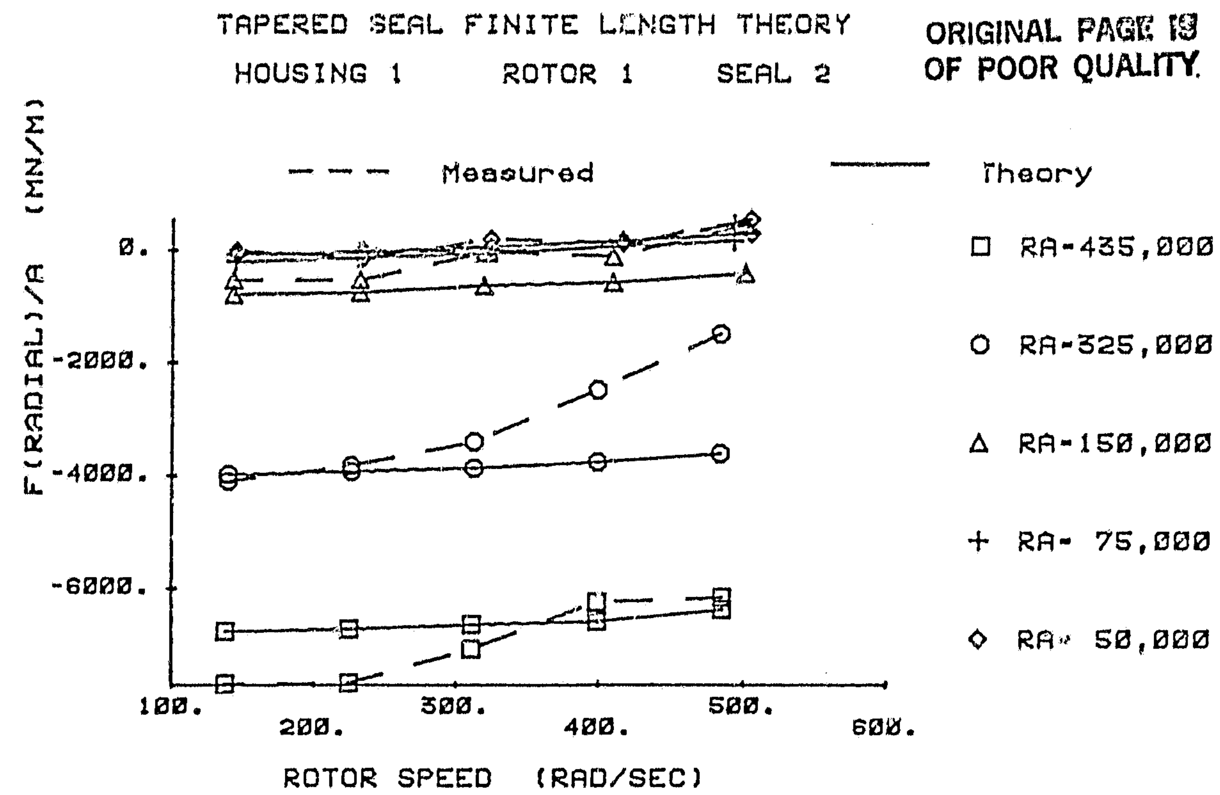

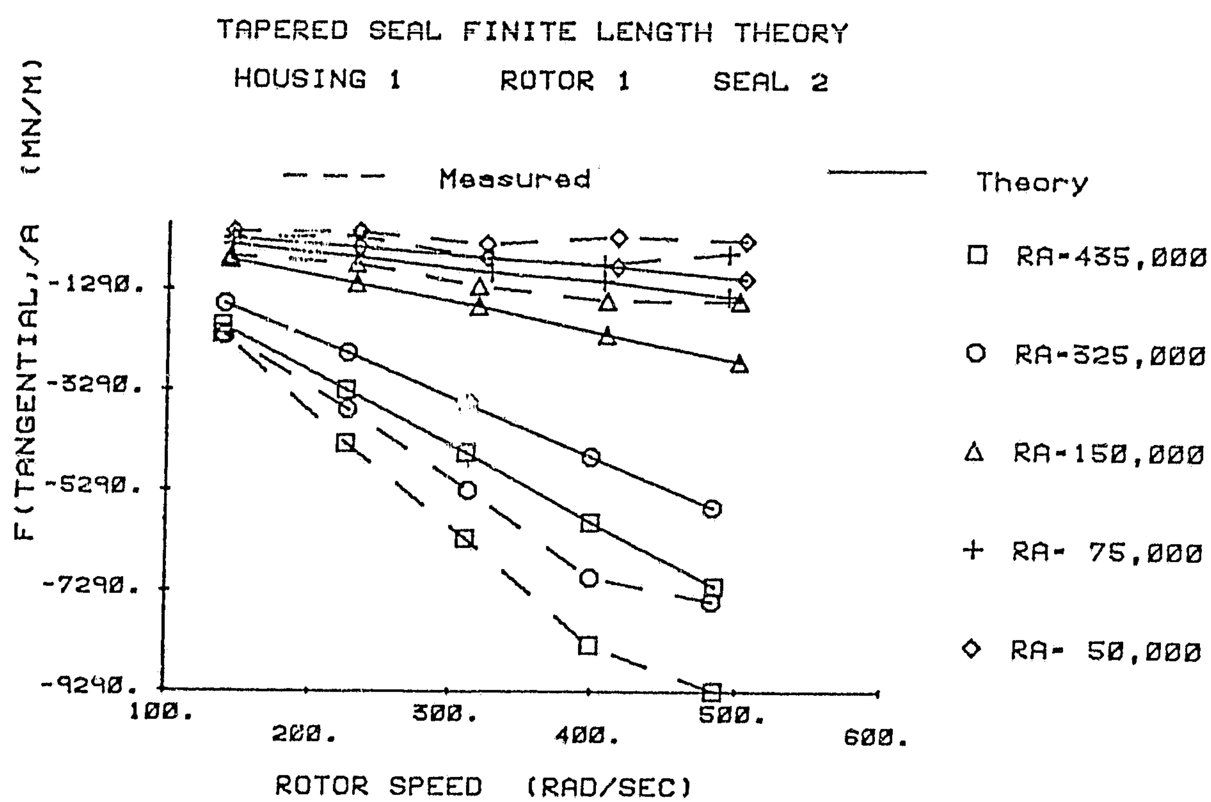

1. F_r/A and F_θ/A versus ω for rotor 1, housing 1. Measured [1] and finite-length theoretical results [4].

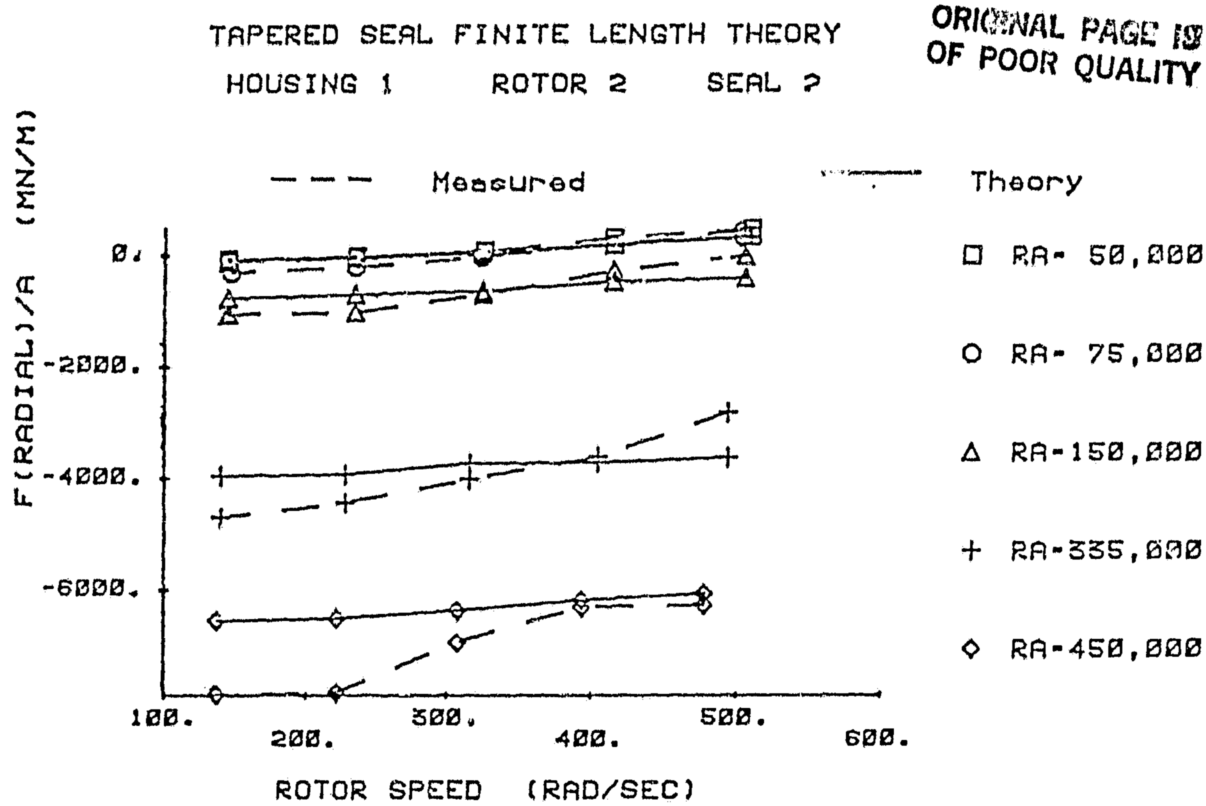

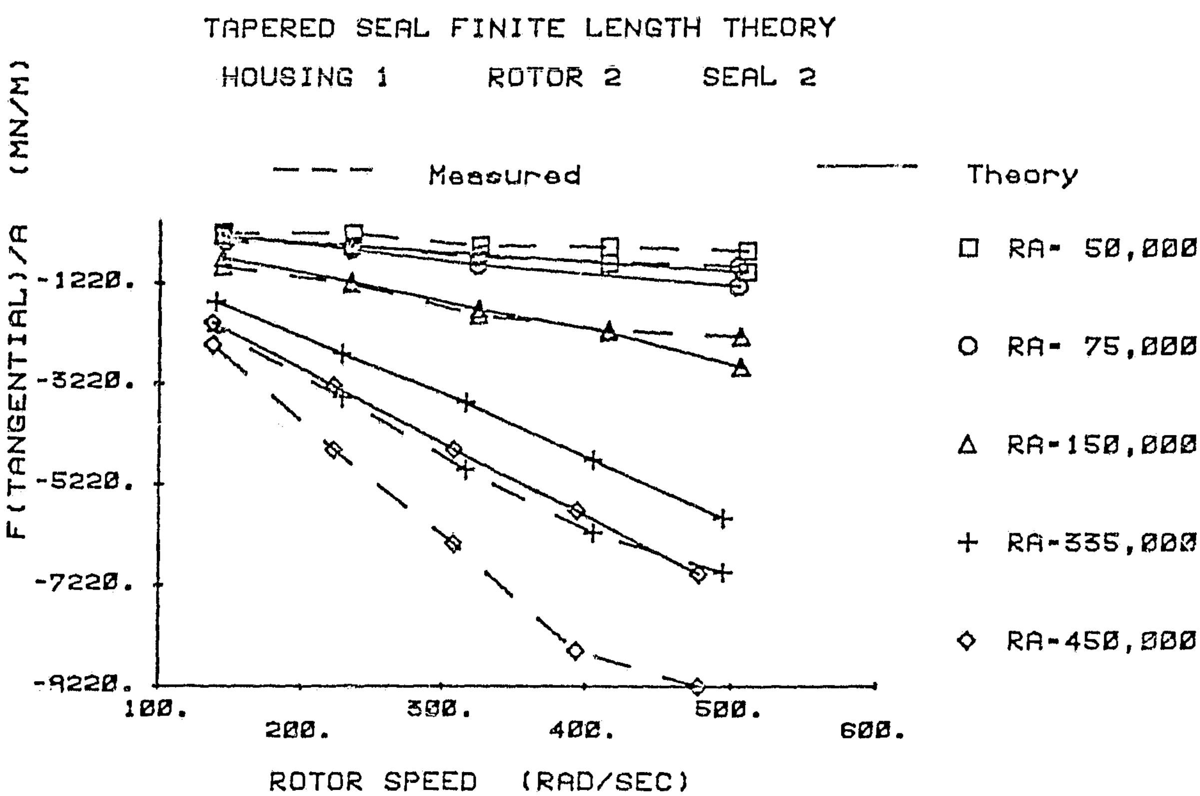

2. F_r/A and F_θ/A versus ω for rotor 2, housing 1. Measured [1] and finite-length theoretical results [4].

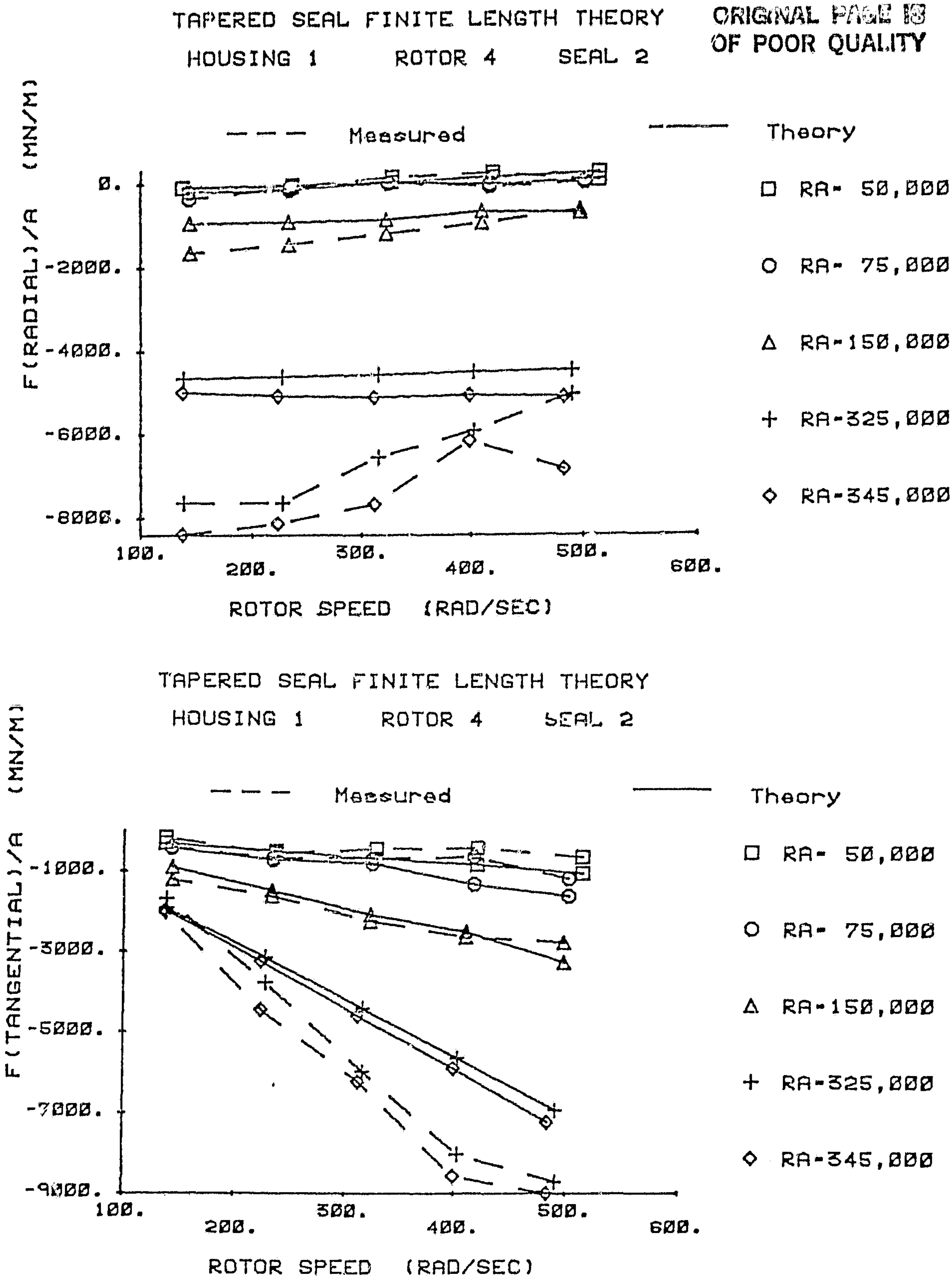

3. F_r/A and F_θ/A versus ω for rotor 4, housing 1. Measured [1] and finite-length theoretical results [4].

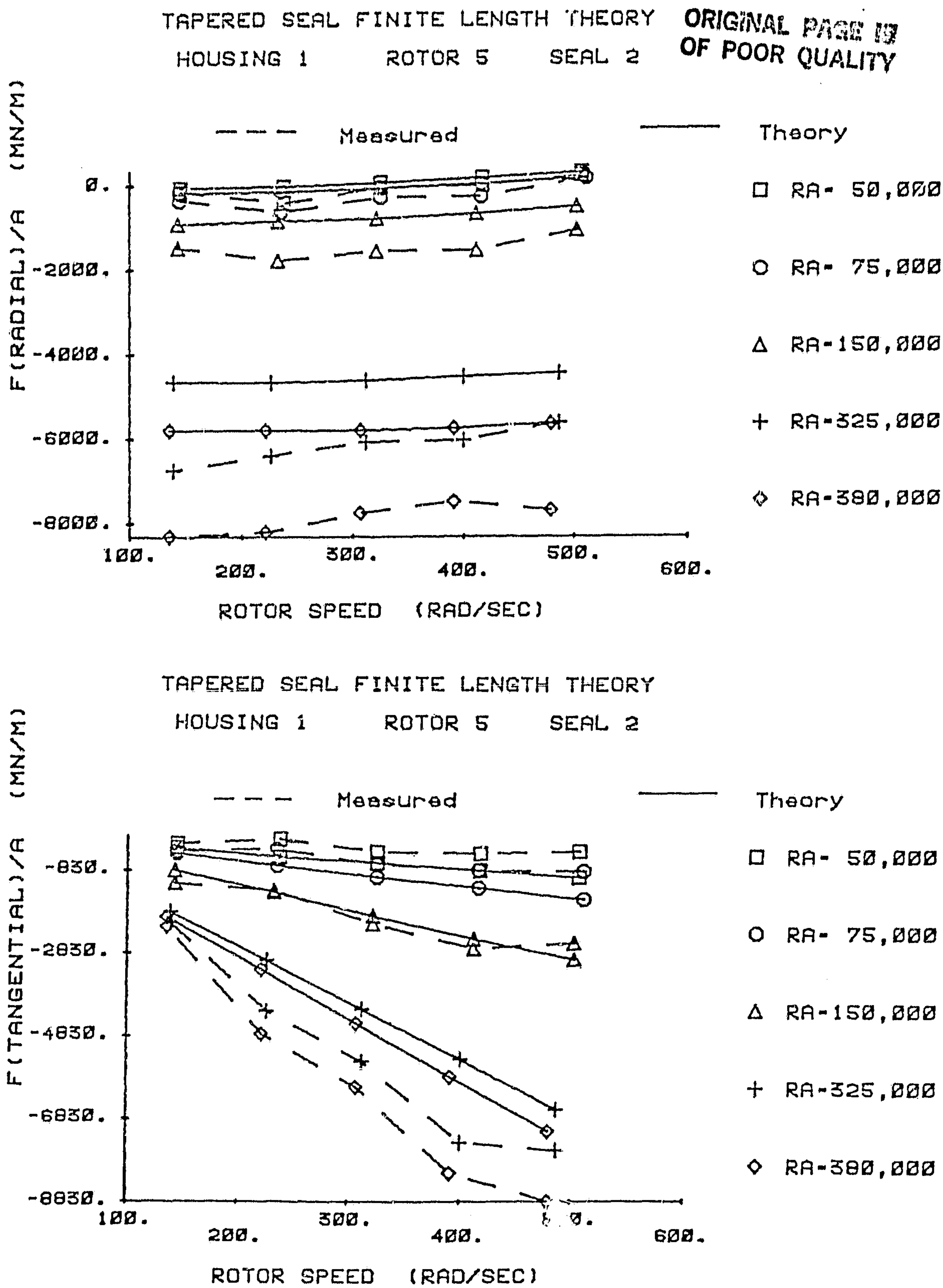

4. F_r/A and F_θ/A versus ω for rotor 5, housing 1. Measured [1] and finite-length theoretical results [4].

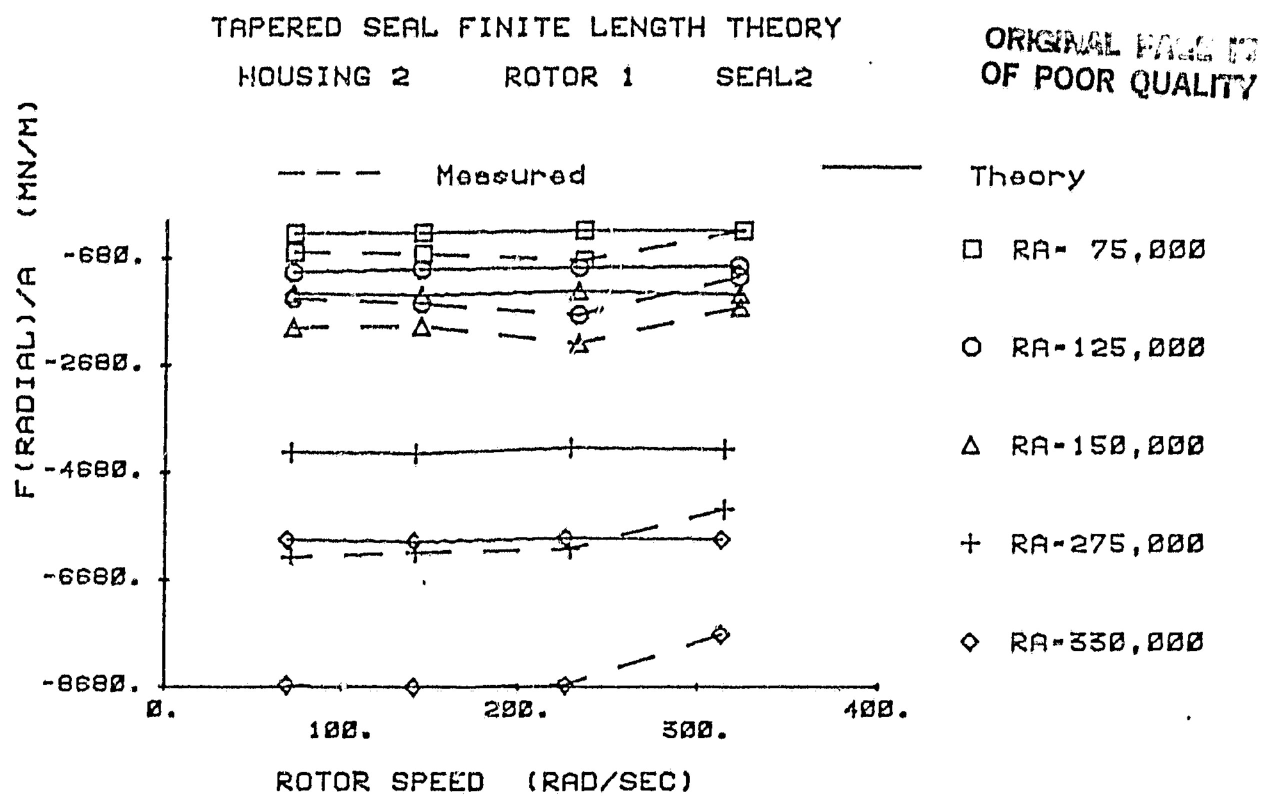

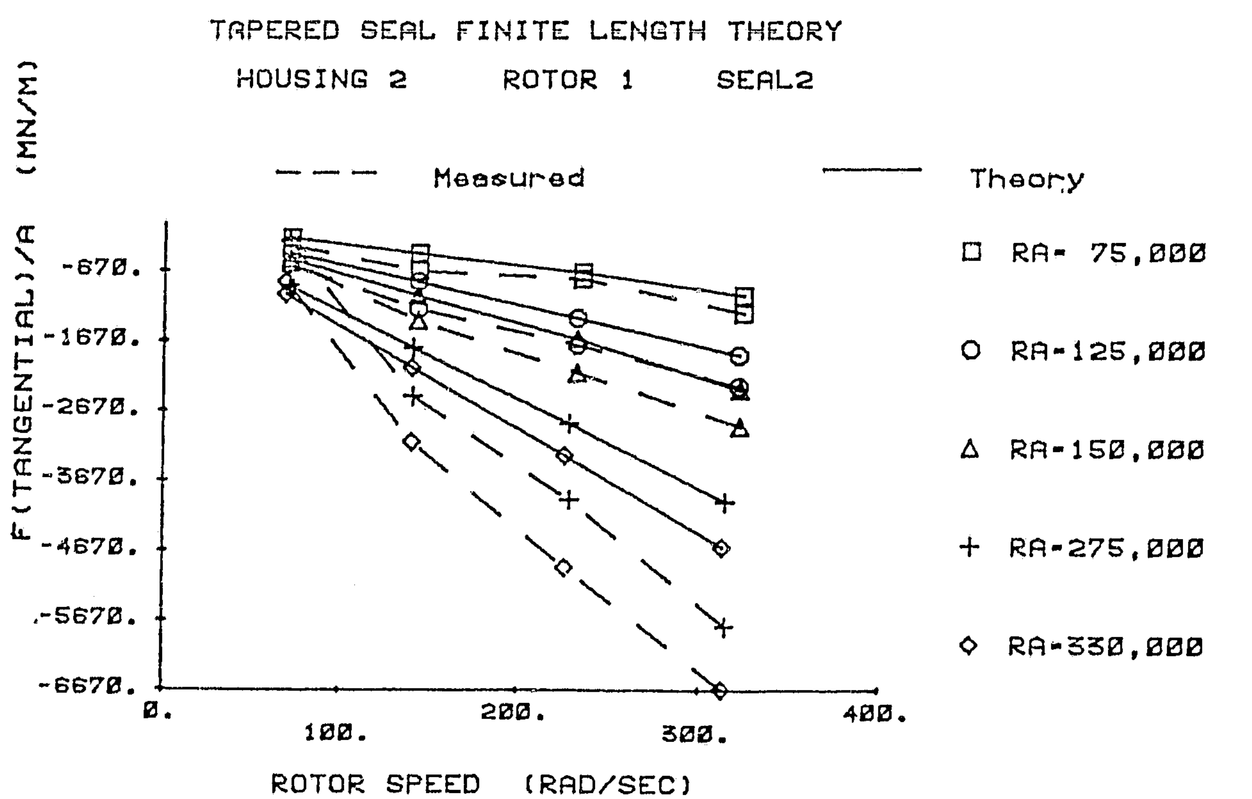

5. F_r/A and F_θ/A versus ω for rotor 1, housing 2. Measured [1] and finite-length theoretical results [4].

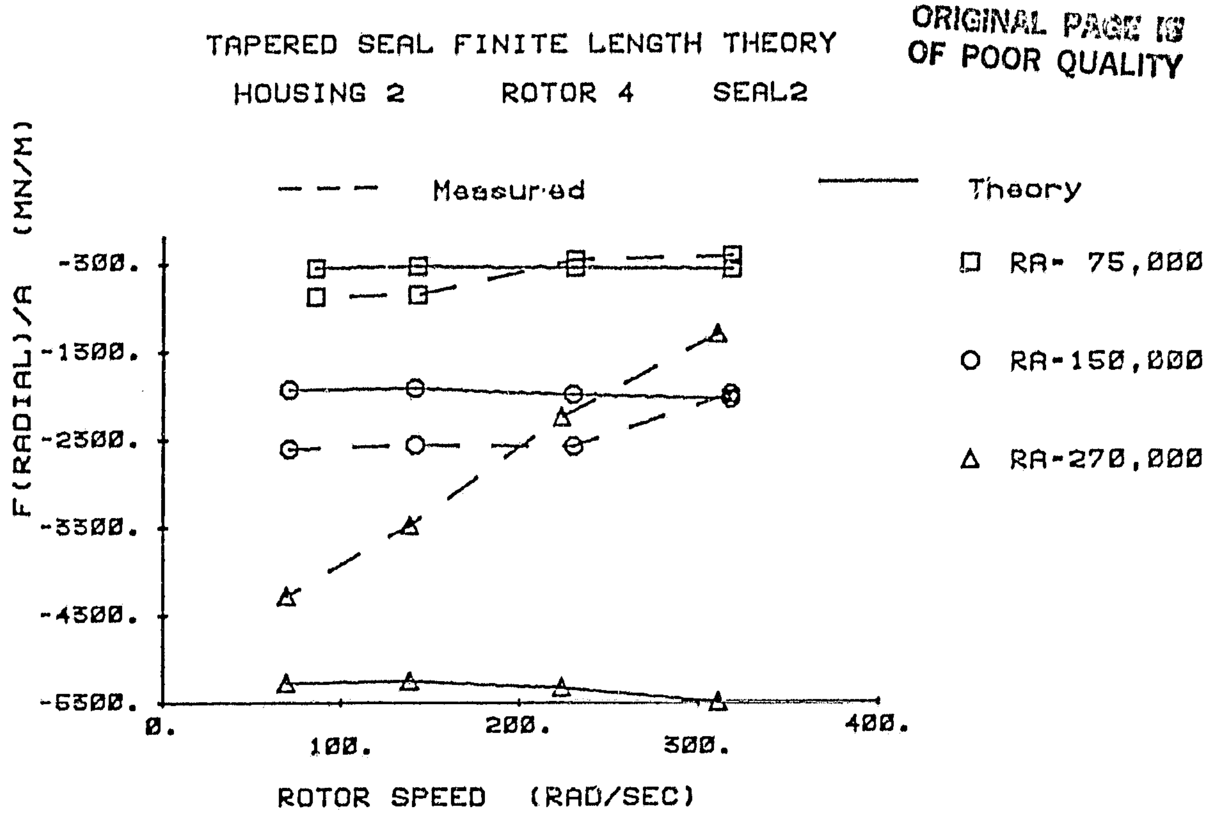

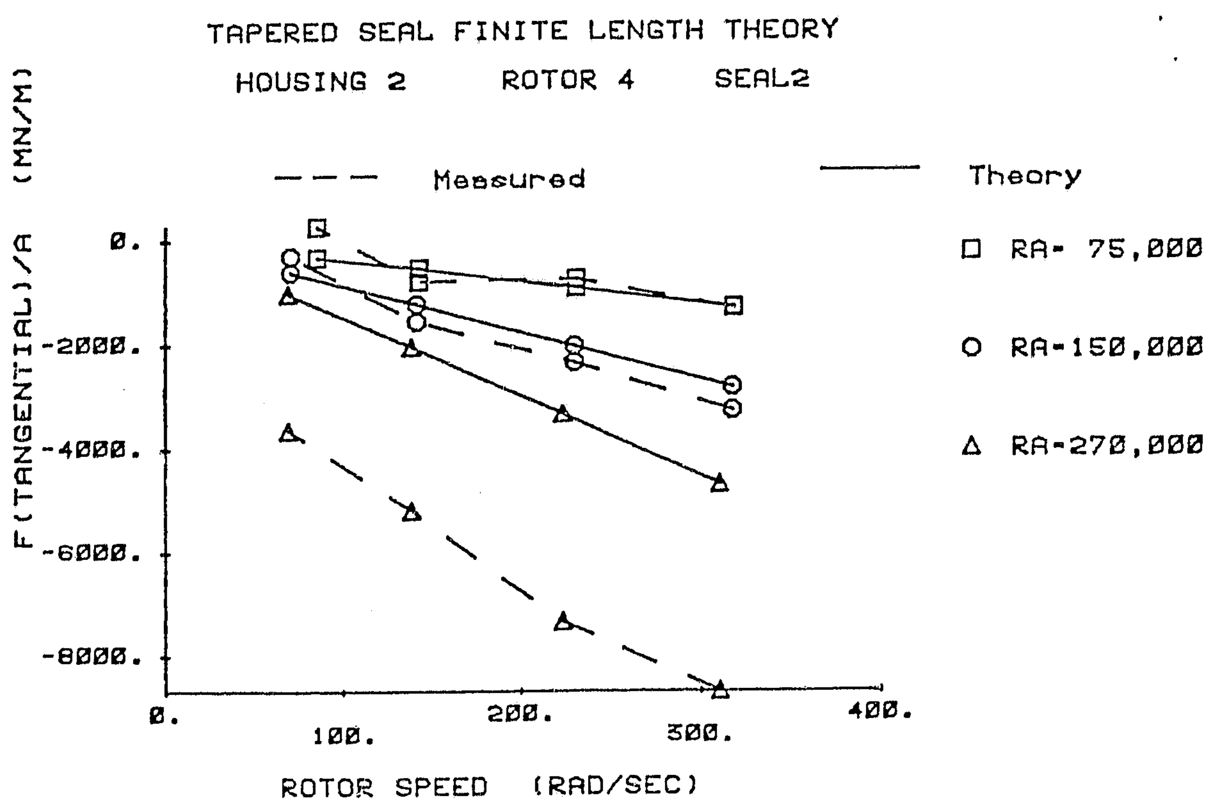

6. F_r/A and F_θ/A versus ω for rotor 4, housing 2. Measured [1] and finite-length theoretical results [4].

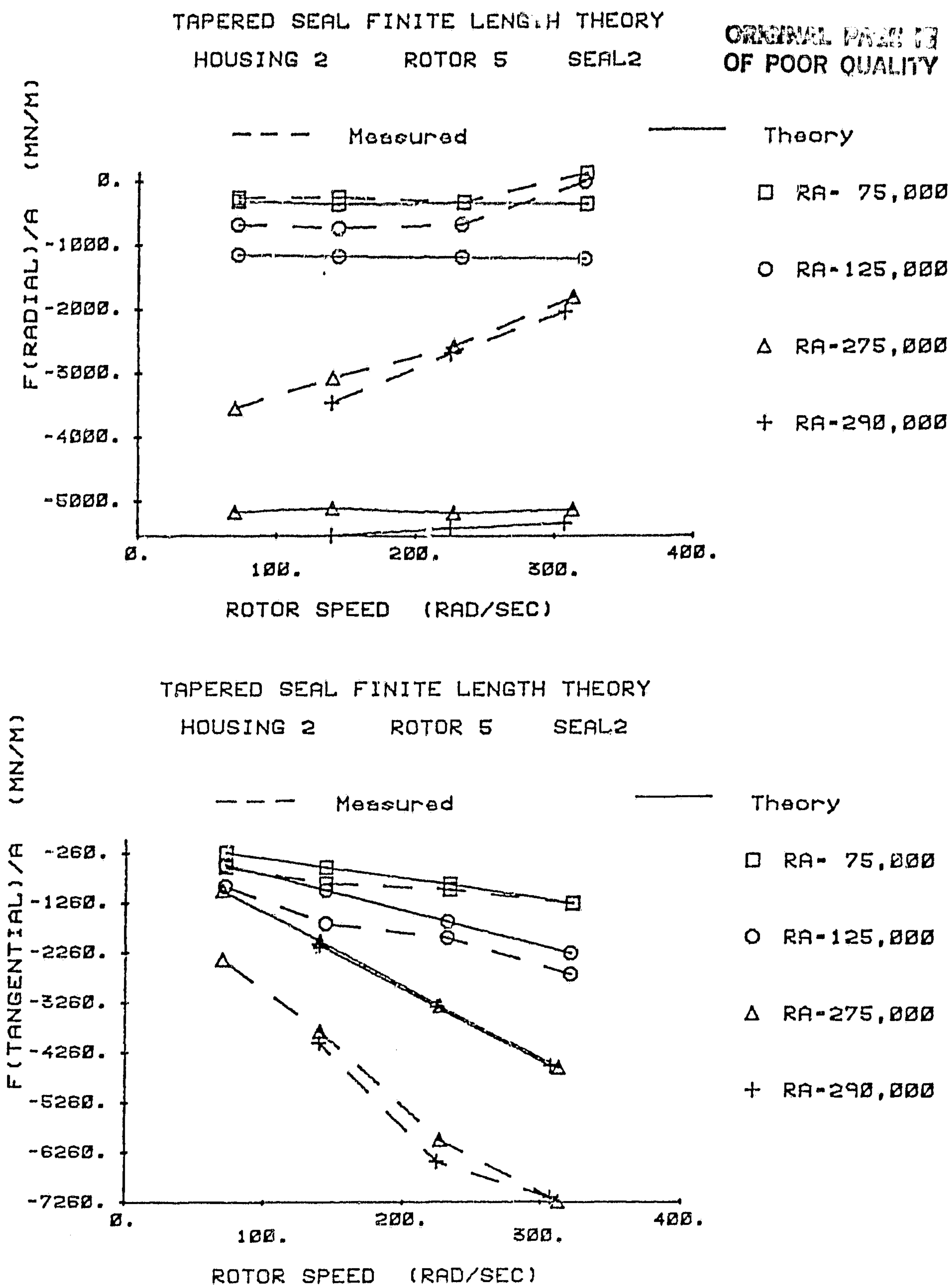

7. F_r/A and F_θ/A versus ω for rotor 5, housing 2. Measured [1] and finite-length theoretical results [4].

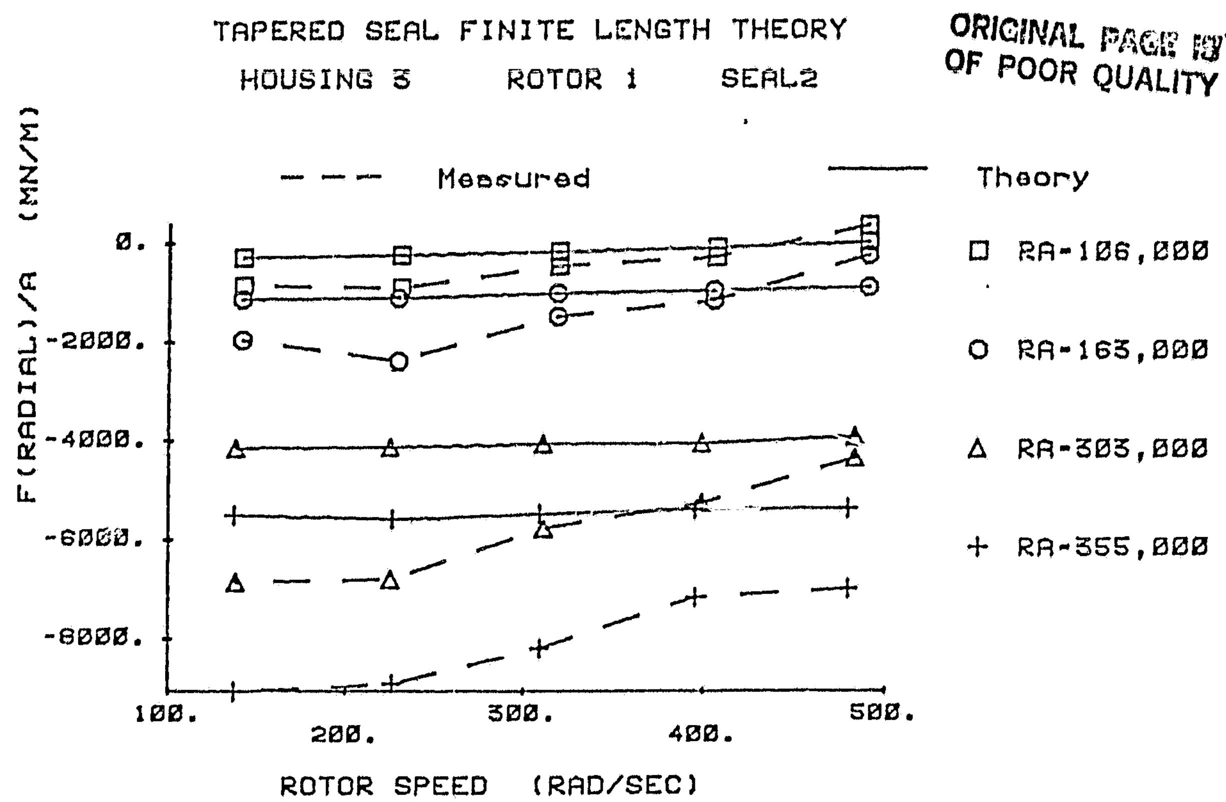

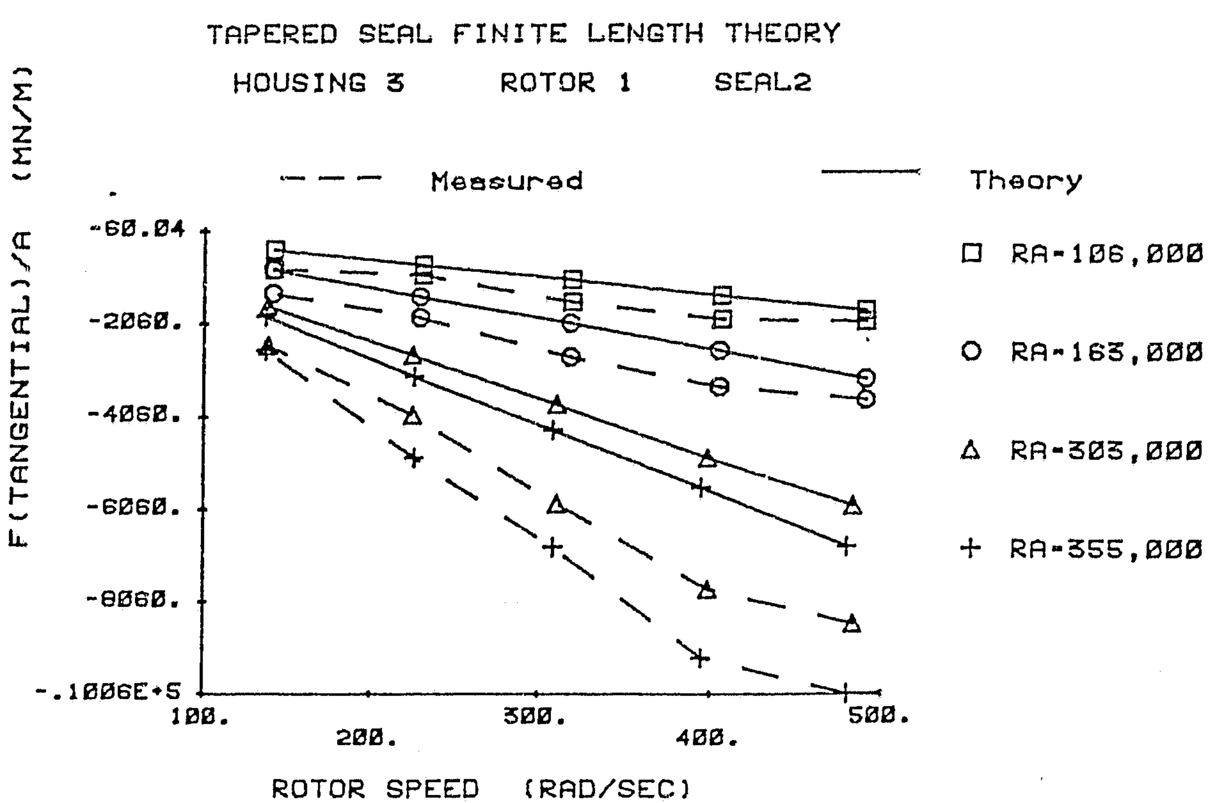

8. F_r/A and F_θ/A versus ω for rotor 1, housing 3. Measured [1] and finite-length theoretical results [4].

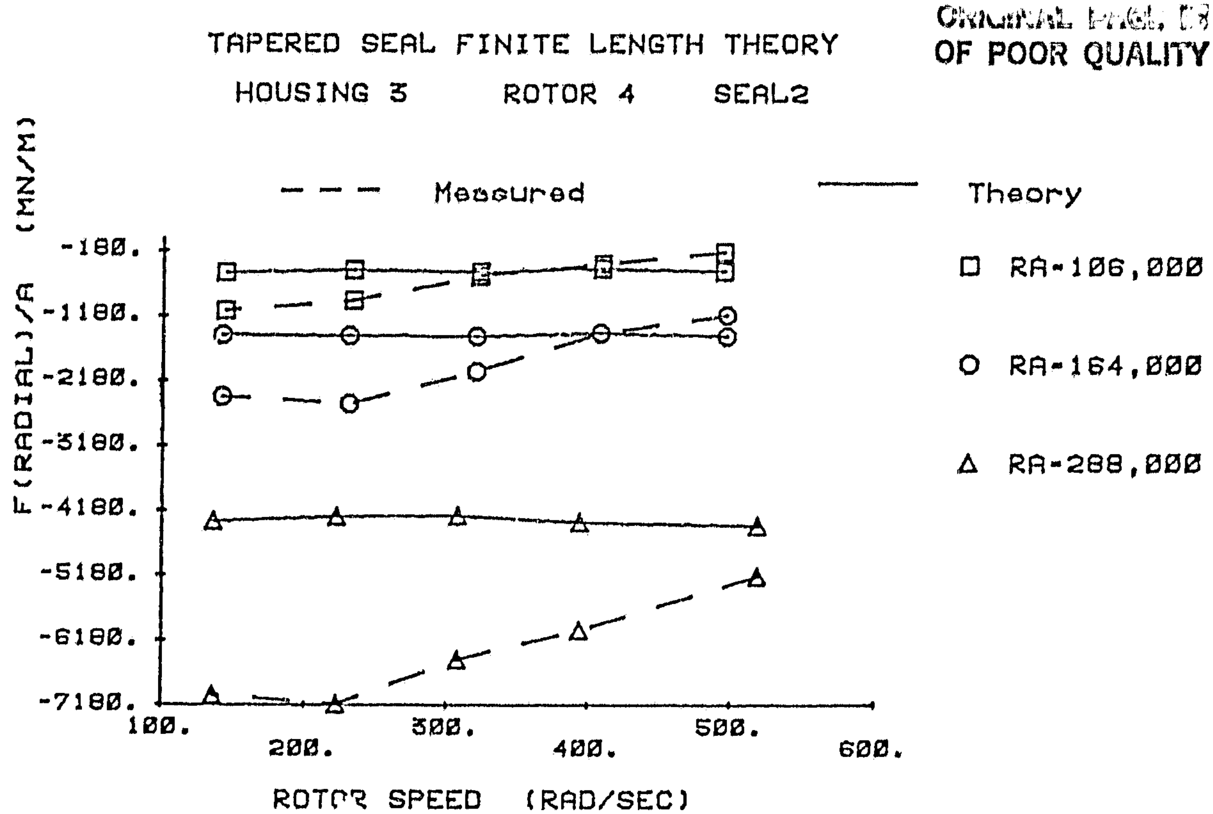

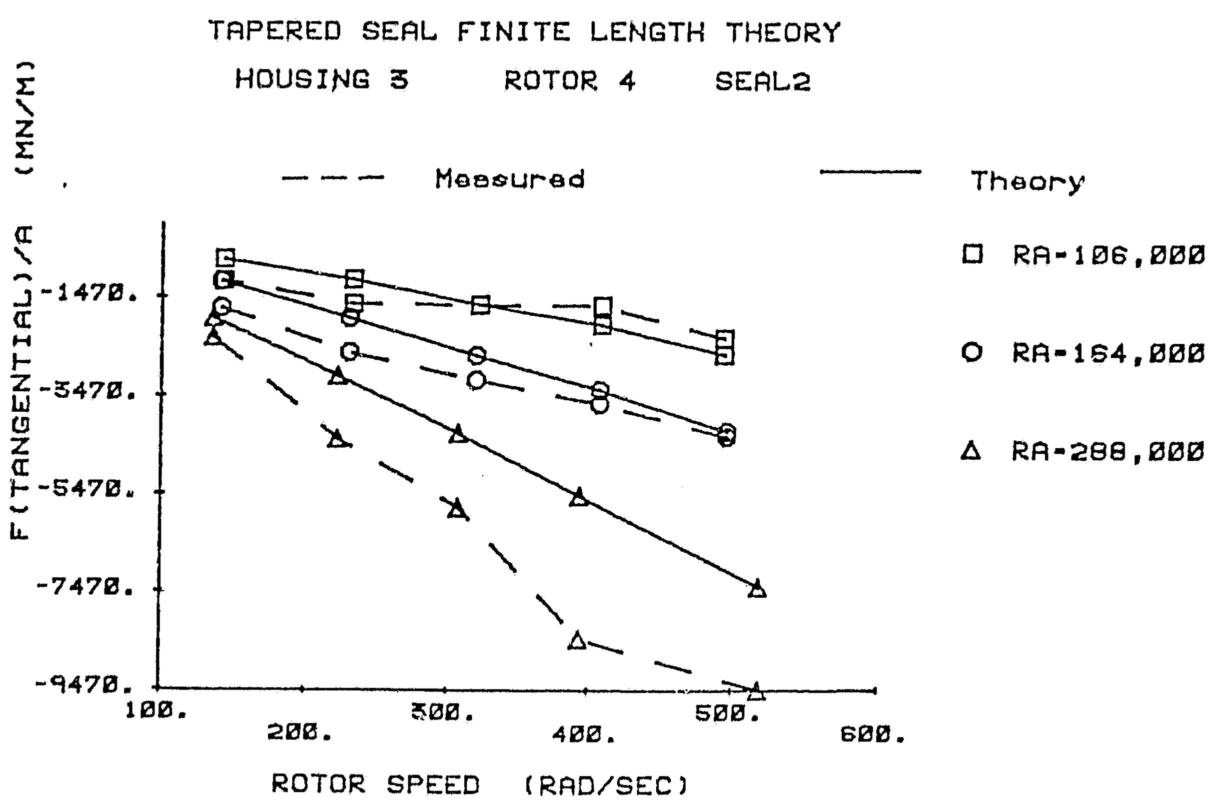

9. F_r/A and F_θ/A versus ω for rotor 4, housing 3. Measured [1] and finite-length theoretical results [4].

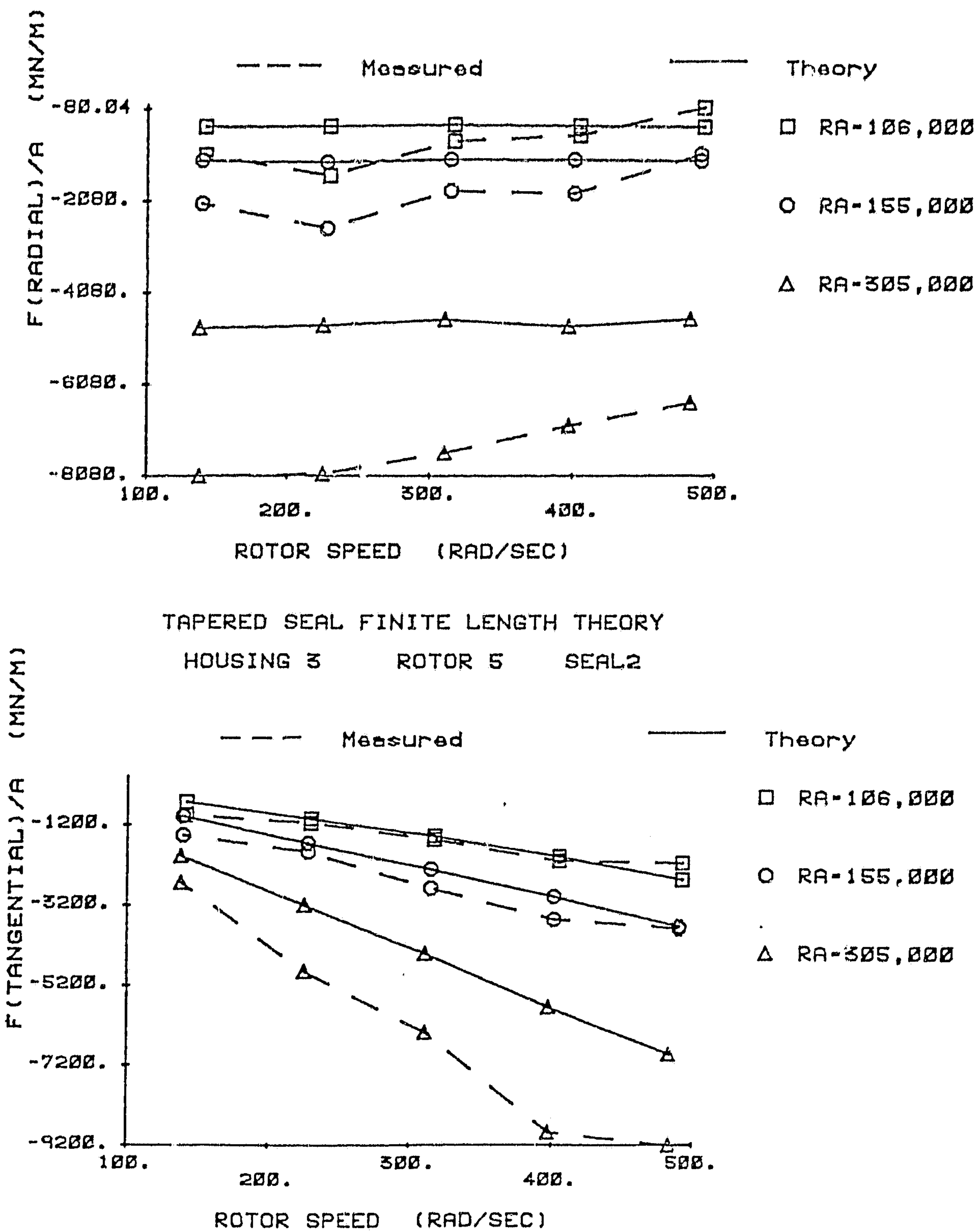

10. F_r/A and F_θ/A versus ω for rotor 5, housing 3. Measured [1] and finite-length theoretical results [4].

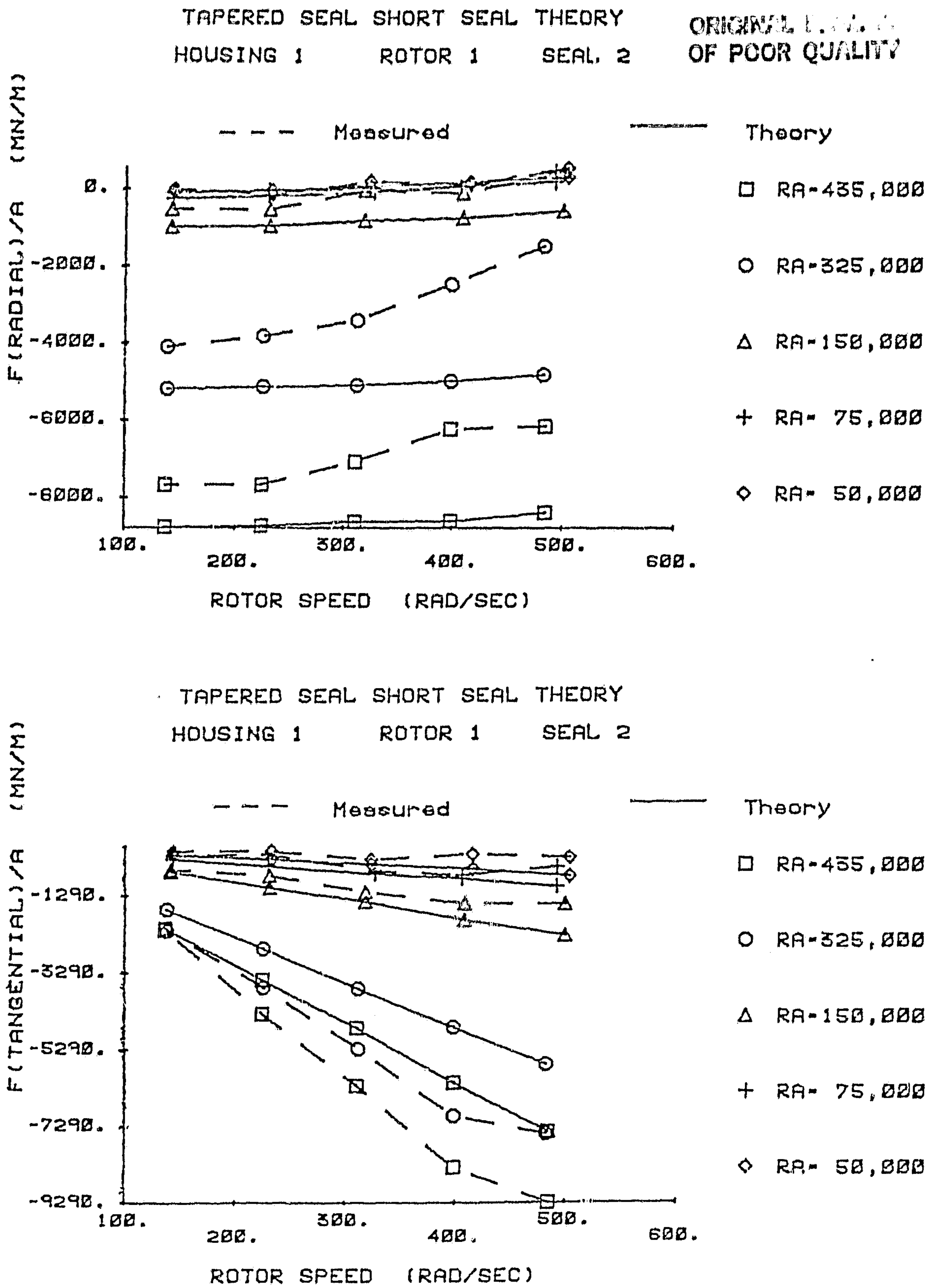

11. F_r/A and F_θ/A versus ω for rotor 1, housing 1. Measured [1] and improved short-seal theoretical results [4].

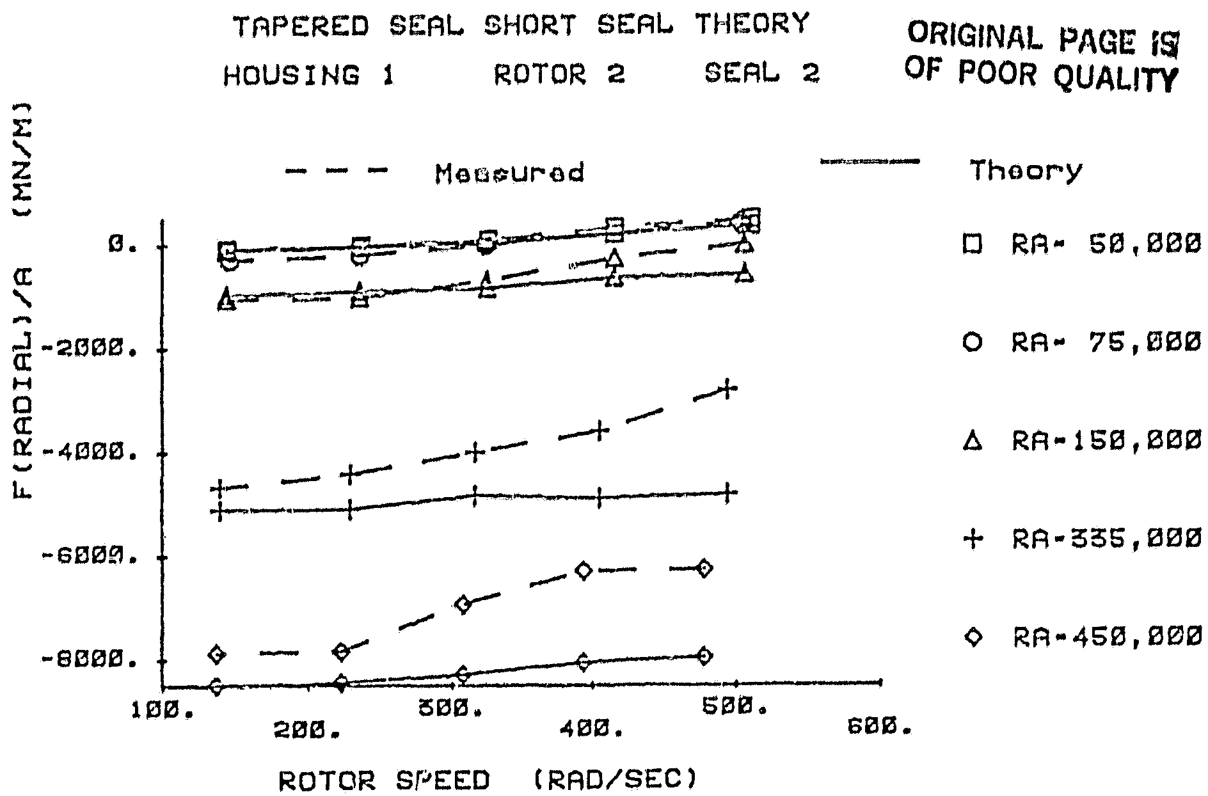

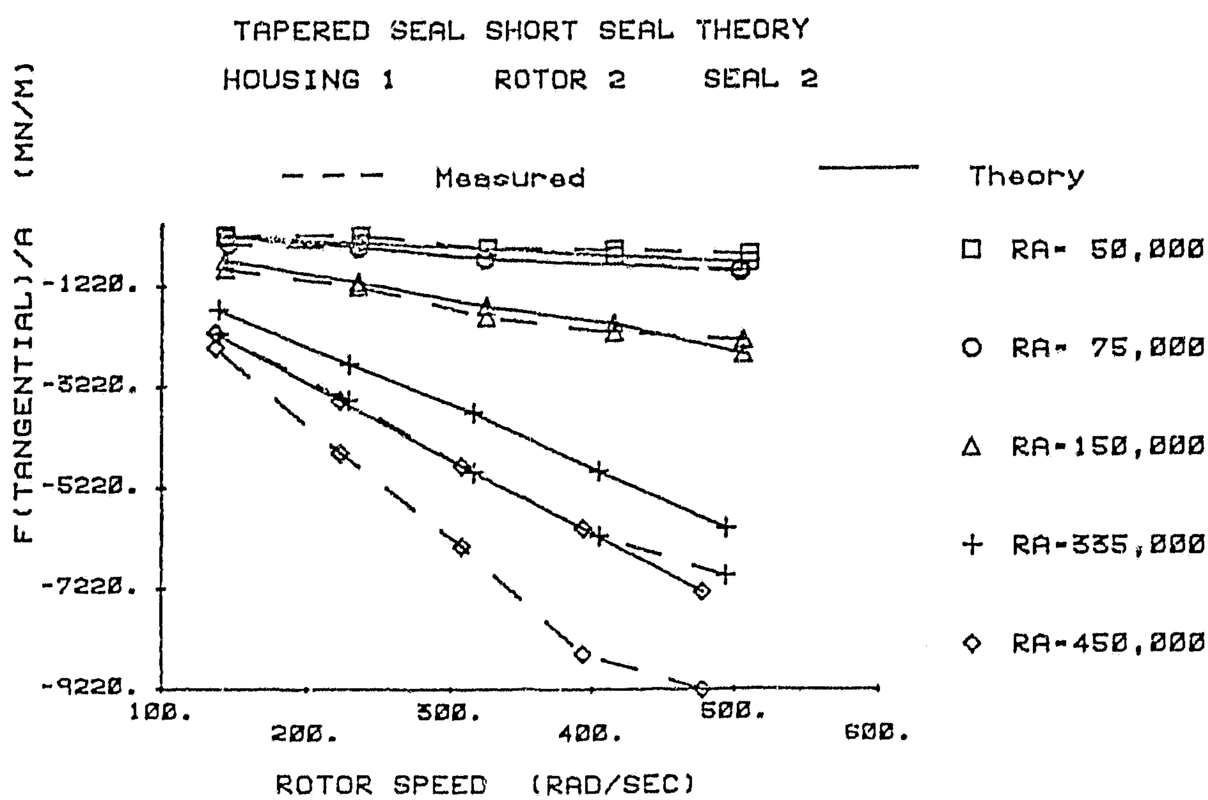

12. F_r/A and F_θ/A versus ω for rotor 2, housing 1. Measured [1] and improved short-seal theoretical results [4].

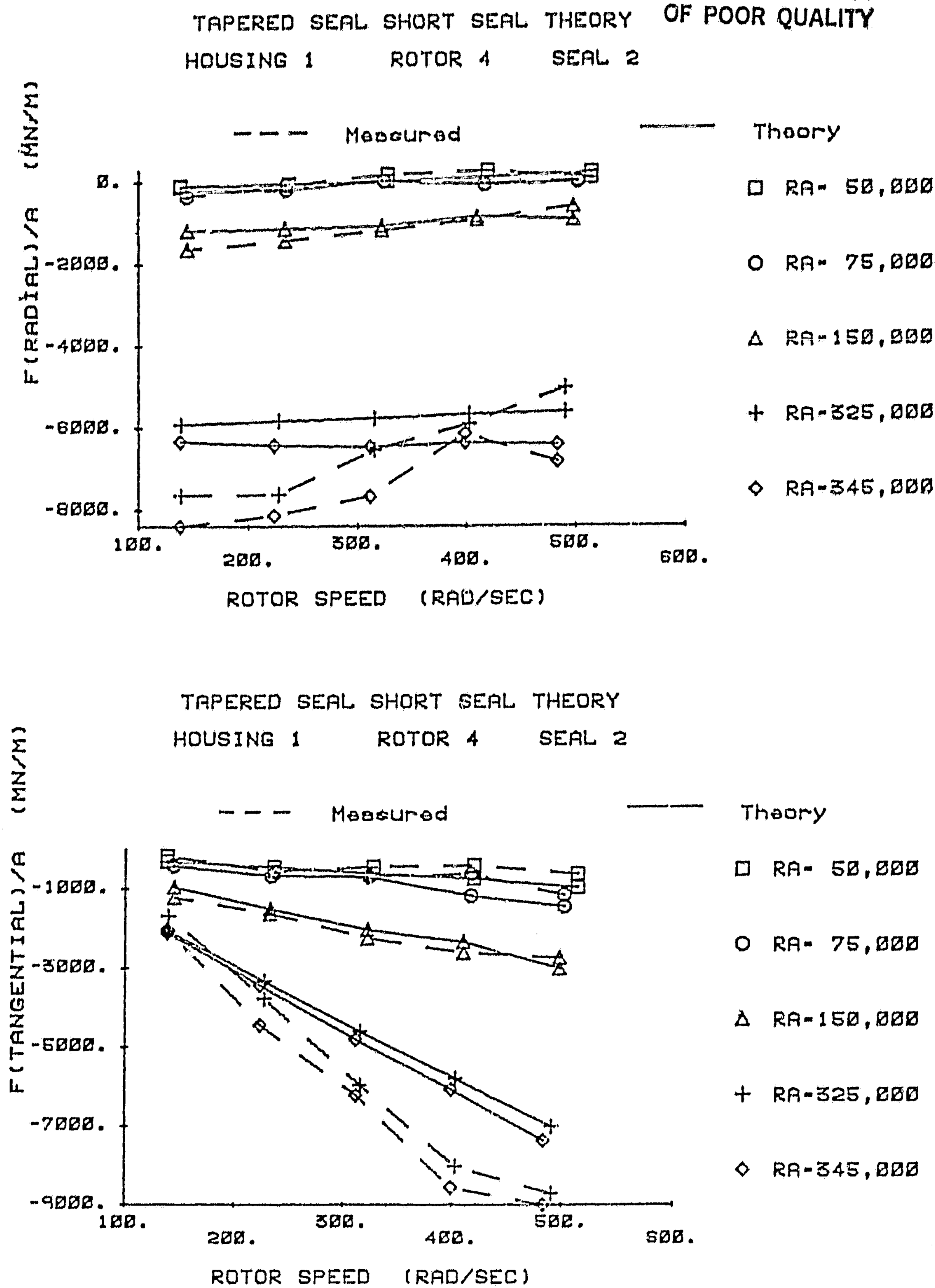

13. F_r/A and F_θ/A versus ω for rotor 4, housing 1. Measured [1] and improved short-seal theoretical results [4].

ORIGINAL PAGE IS
OF POOR QUALITY

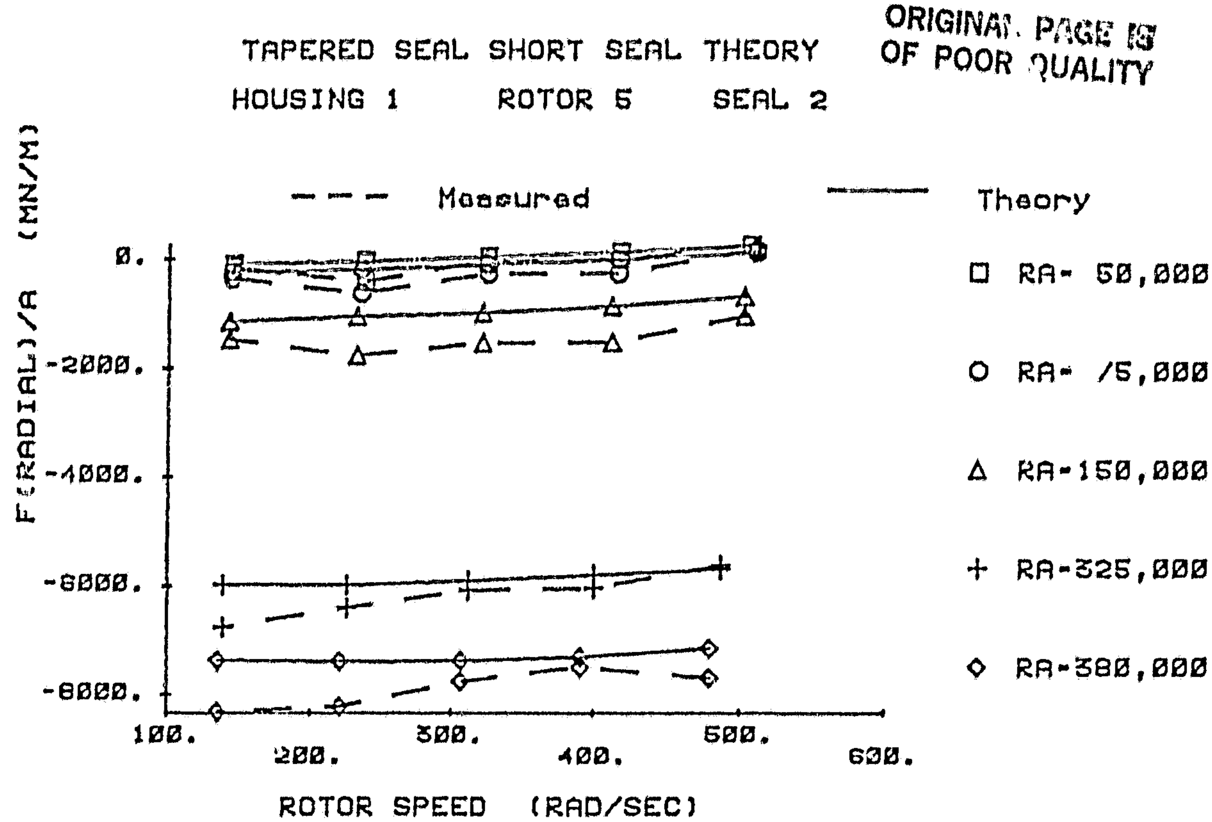

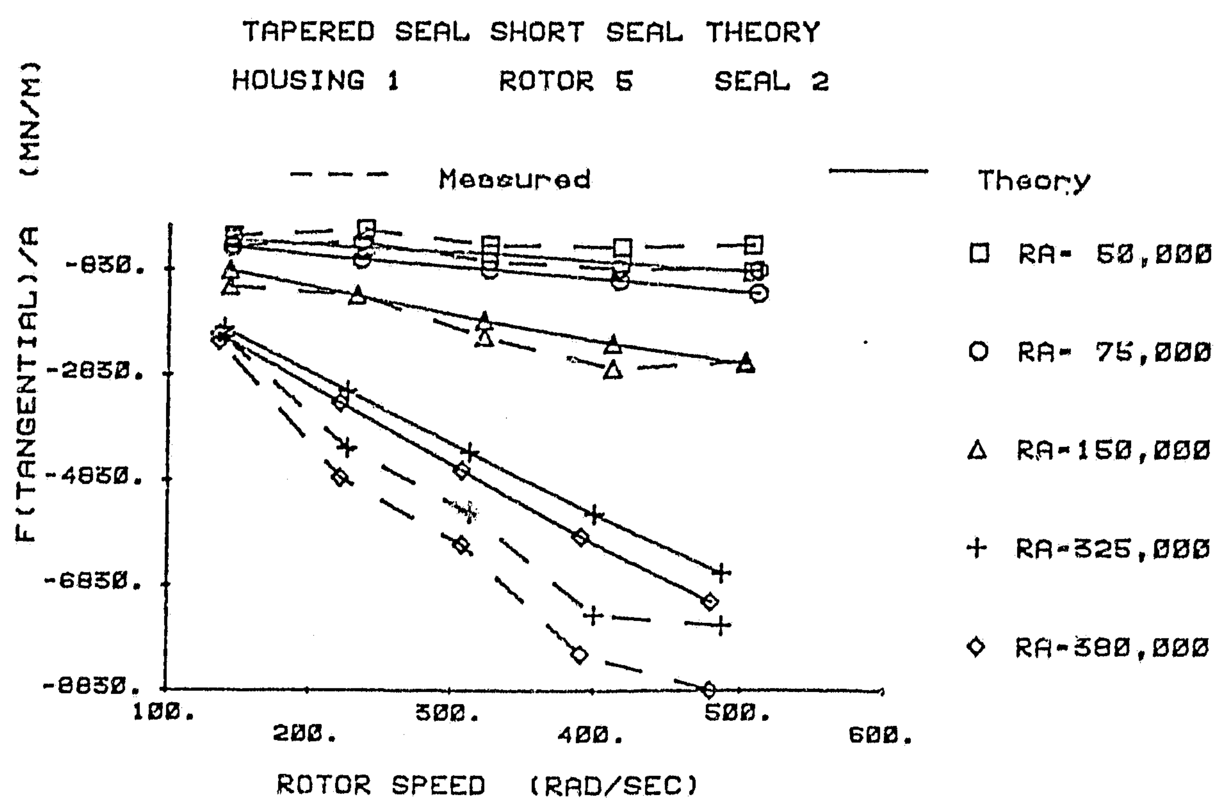

14. F_r/A and F_θ/A versus ω for rotor 5, housing 1. Measured [1] and improved short-seal theoretical results [4].

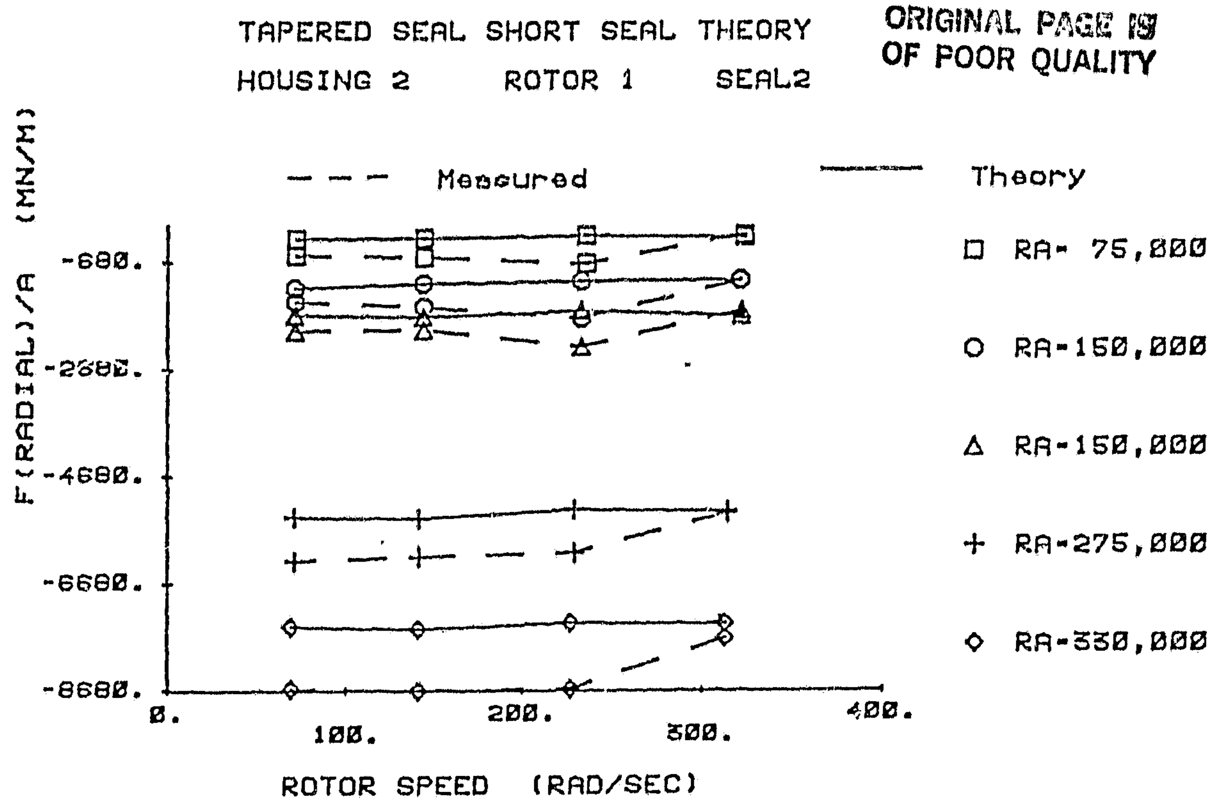

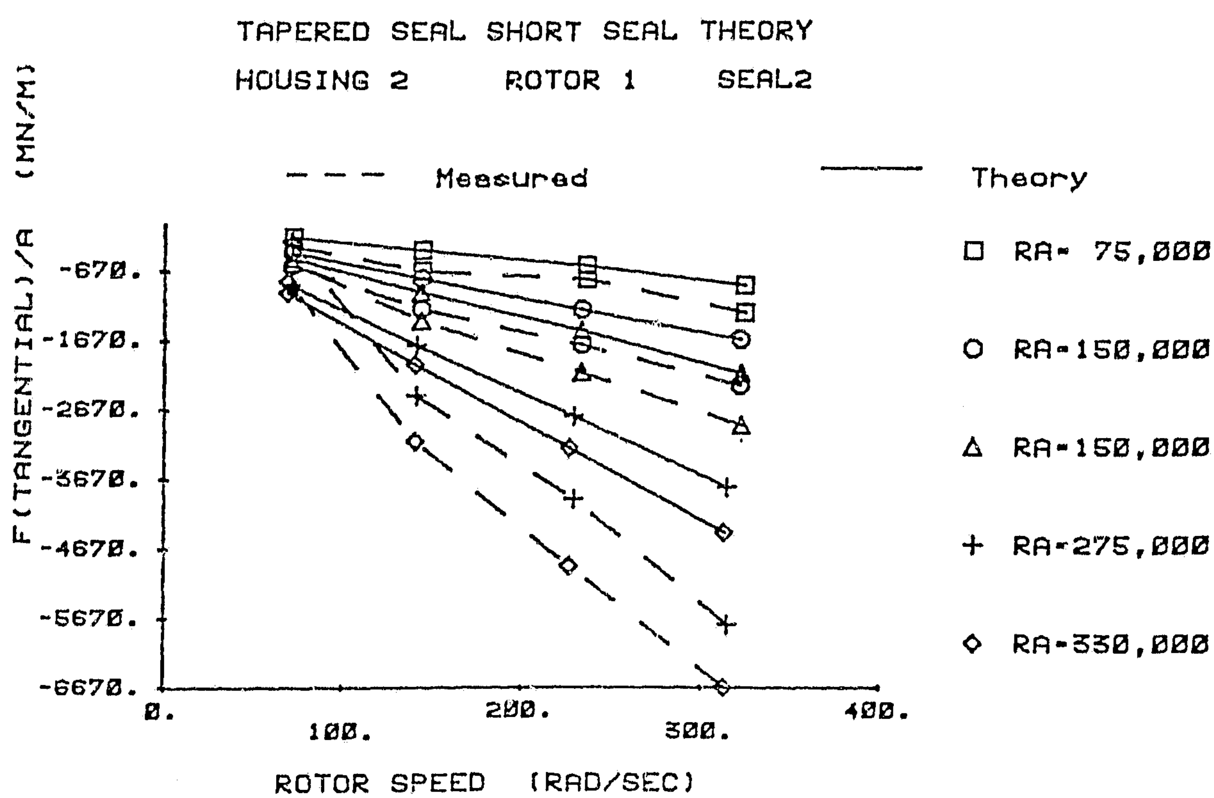

15. F_r/A and F_θ/A versus ω for rotor 1, housing 2. Measured [1] and improved short-seal theoretical results [4].

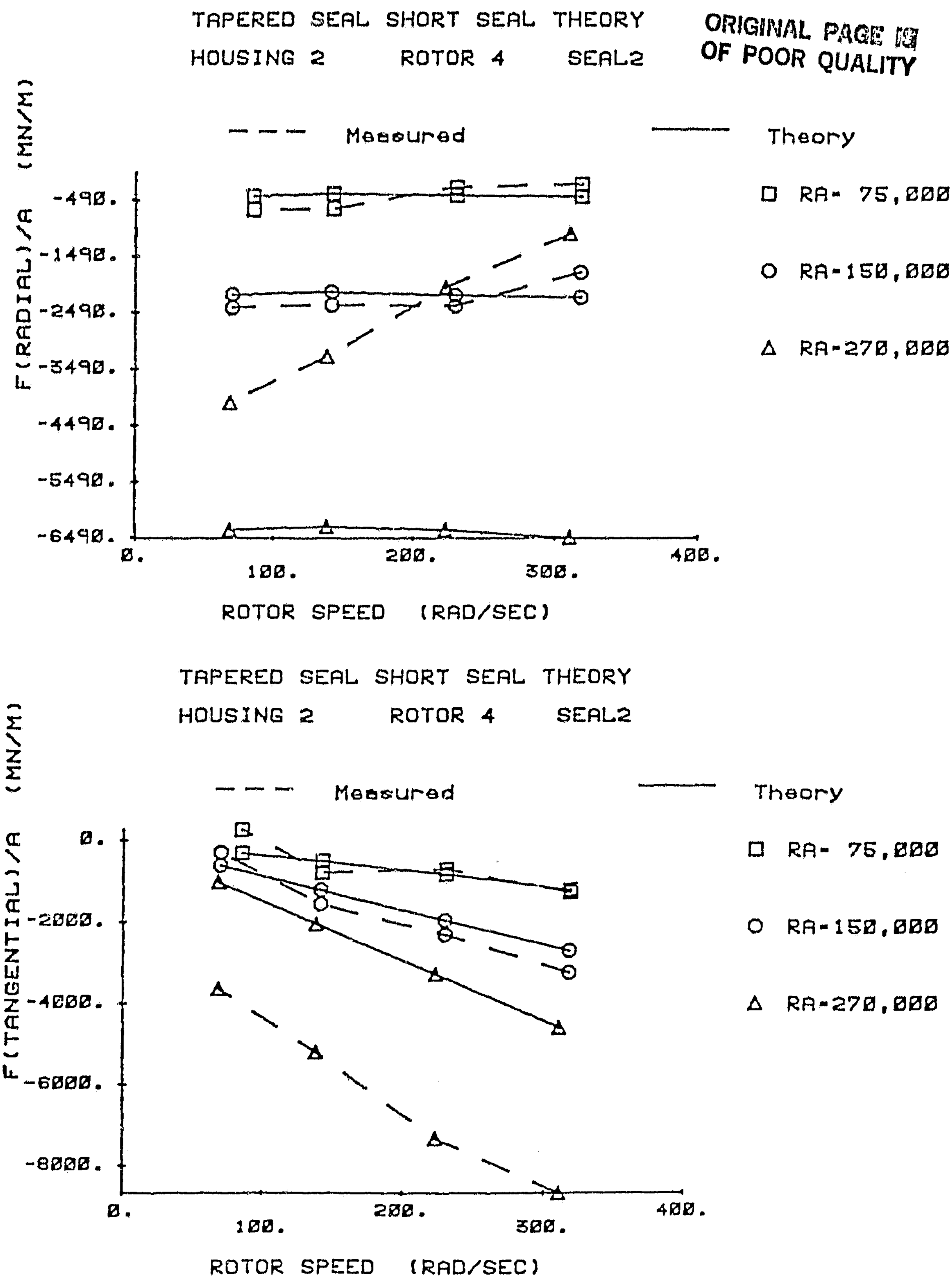

16. F_r/A and F_θ/A versus ω for rotor 4, housing 2. Measured [1] and improved short-seal theoretical result [4].

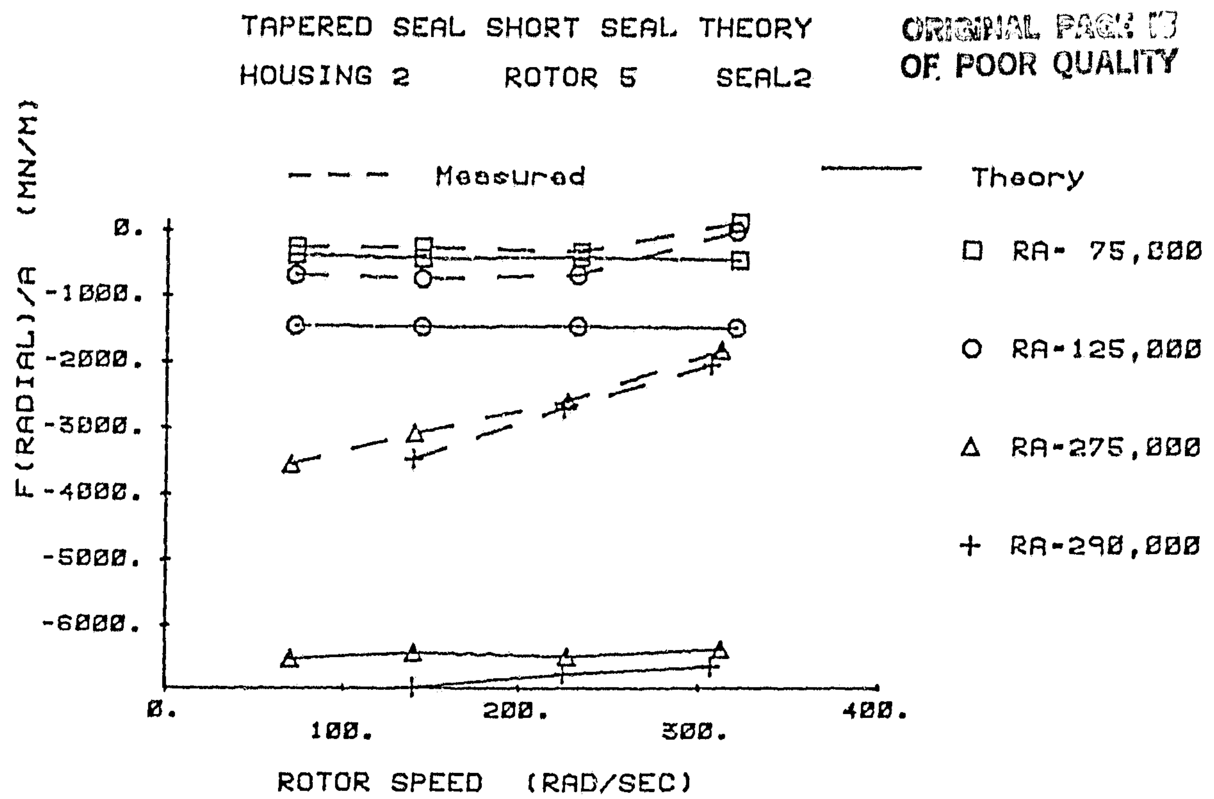

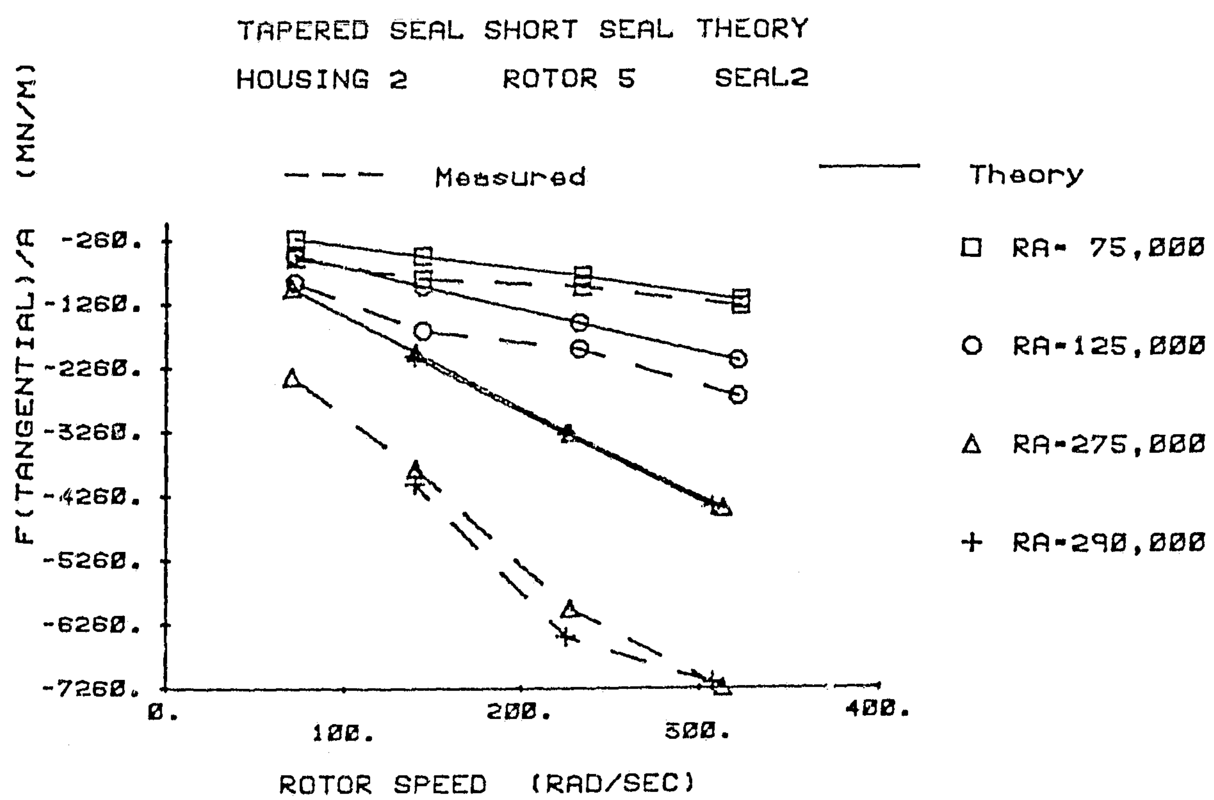

17. F_r/A and F_θ/A versus ω for rotor 5, housing 2. Measured [1] and improved short-seal theoretical results [4].

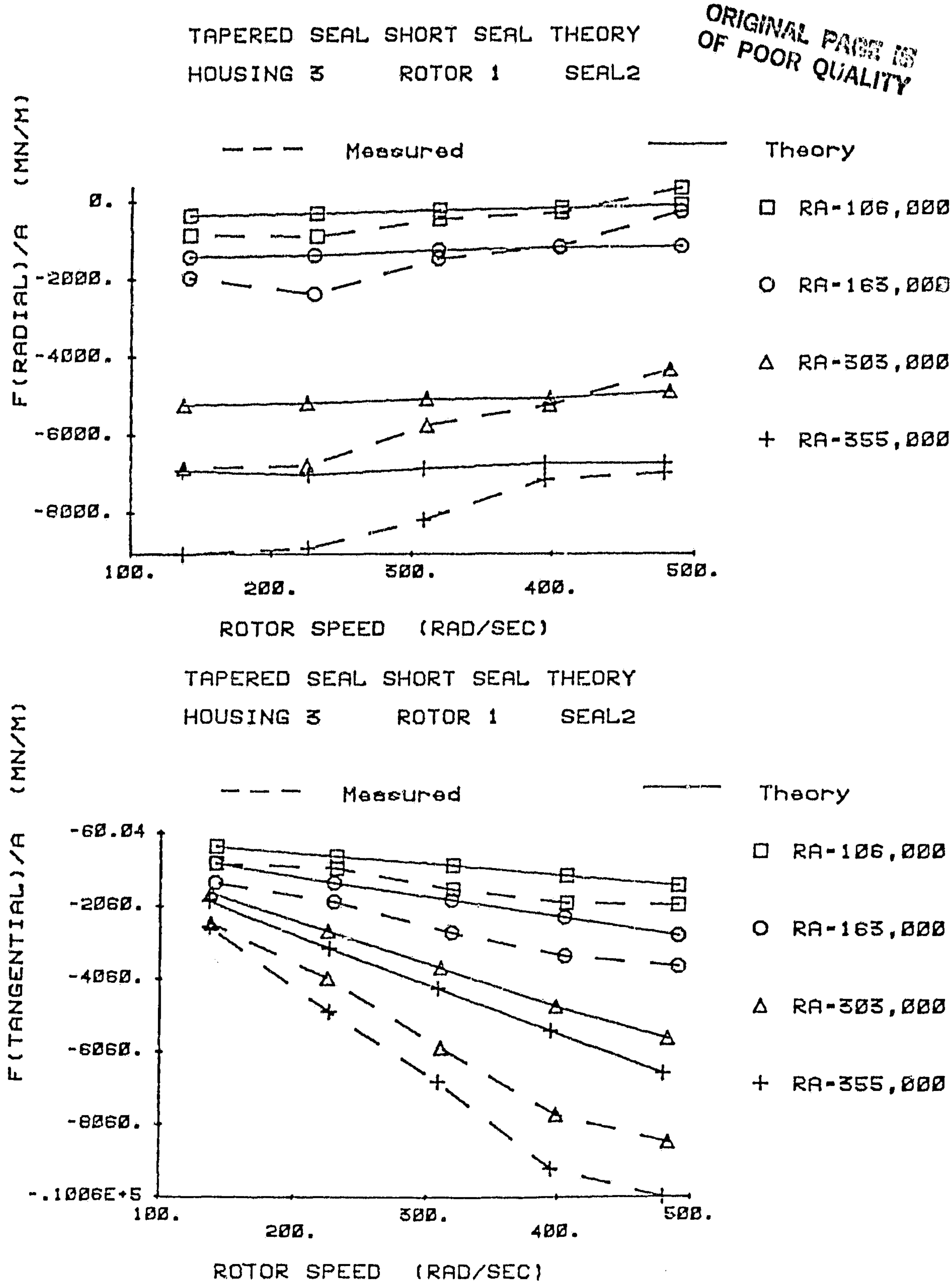

18. F_r/A and F_θ/A versus ω for rotor 1, housing 3. Measured [1] and improved short-seal theoretical results [4].

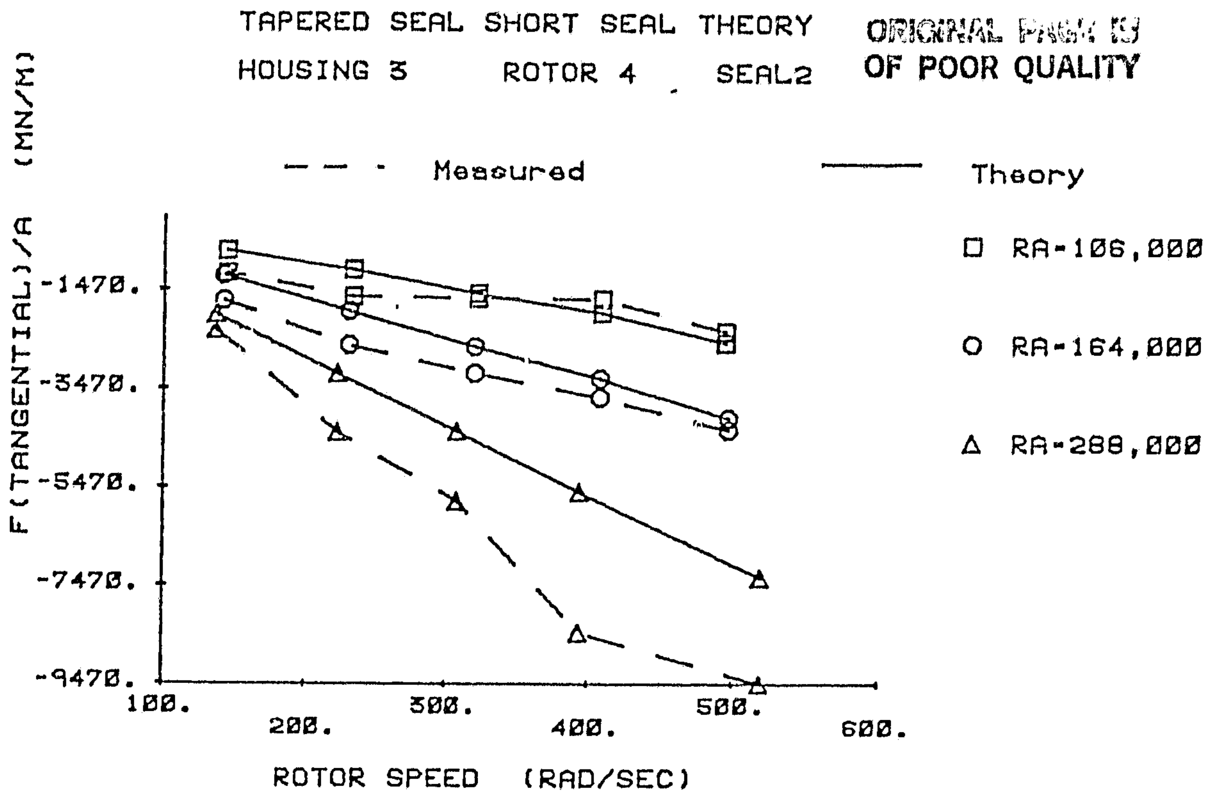

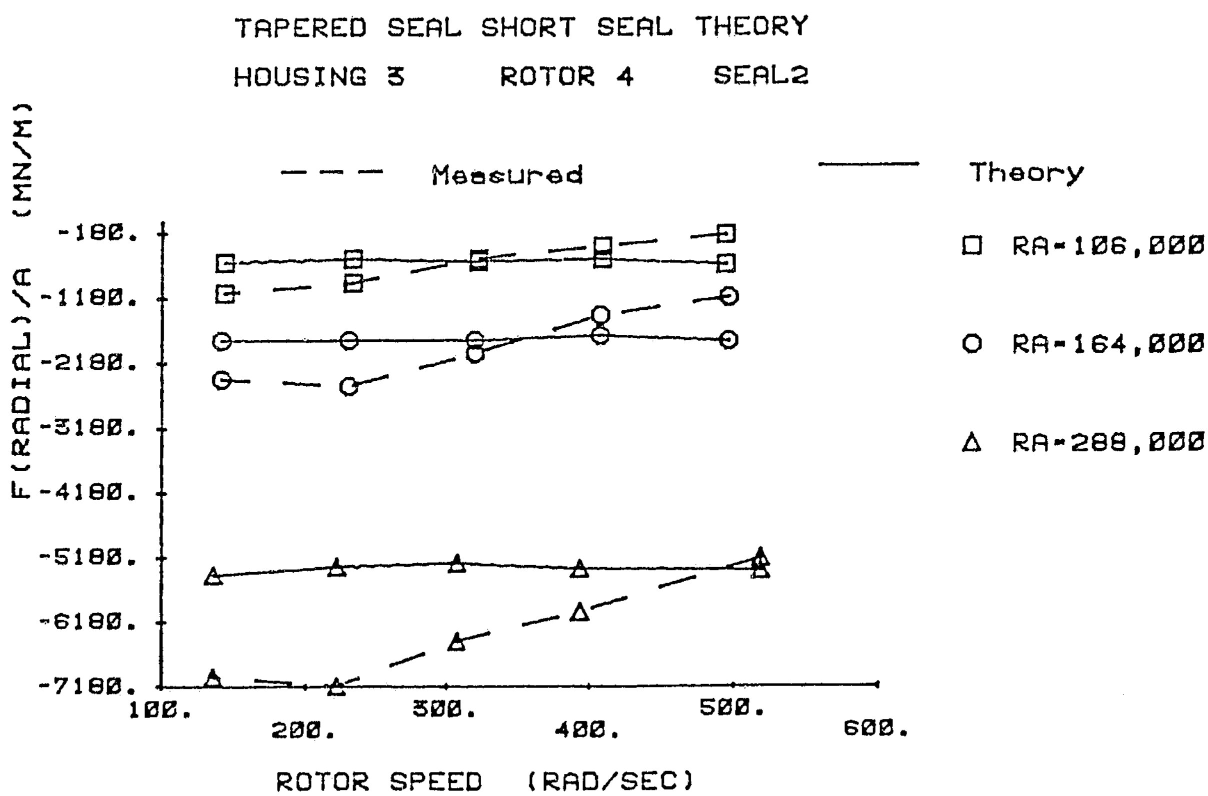

19. F_r/A and F_θ/A versus ω for rotor 4, housing 3. Measured [1] and improved short-seal theoretical results [4].

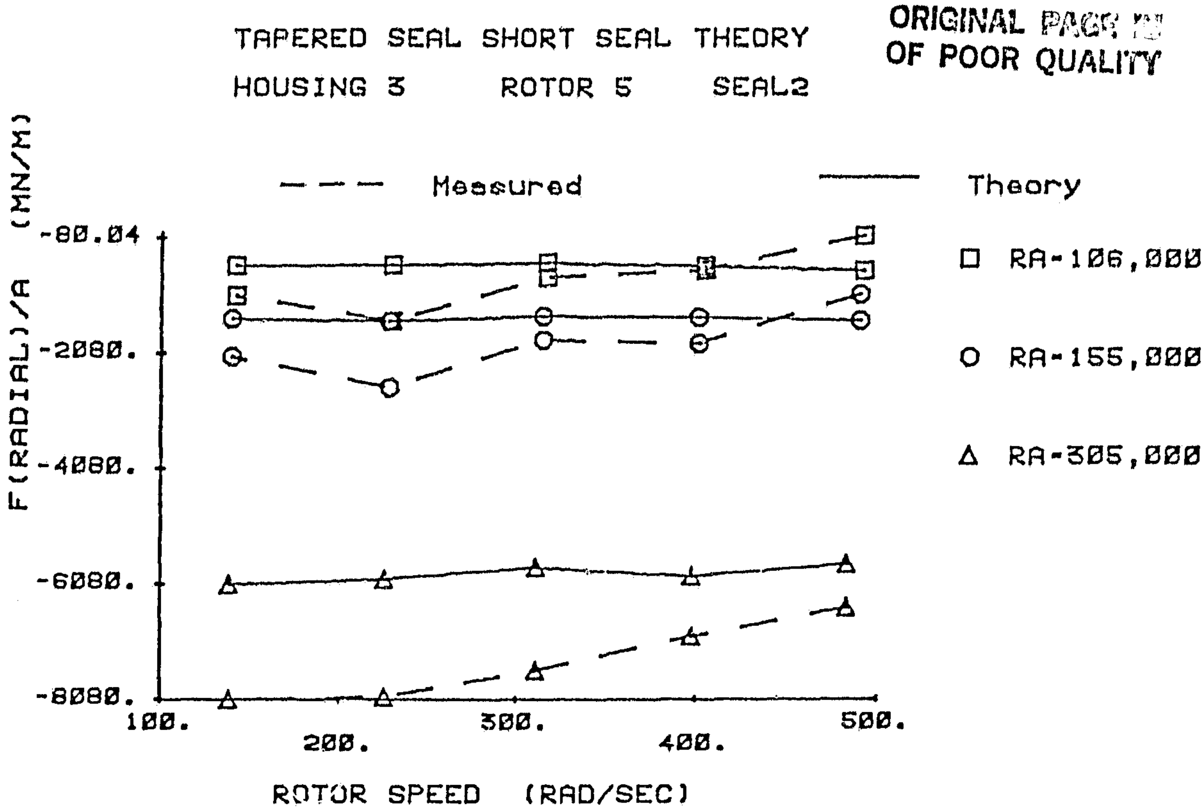

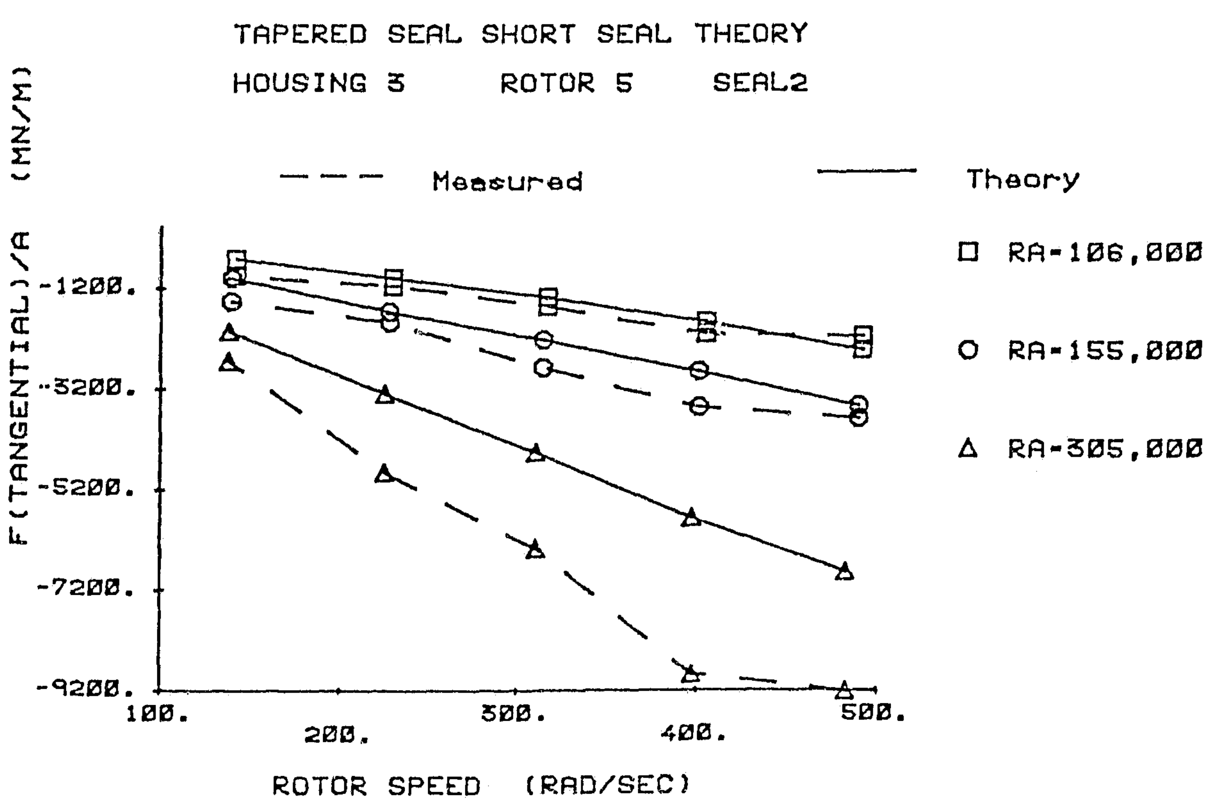

20. F_r/A and F_θ/A versus ω for rotor 5, housing 3. Measured [1] and improved short-seal theoretical results [4].

TAPERED SEAL FINITE LENGTH THEORY SEAL 2 (TAPERED)
SI UNITS

	KEF(EXP)	KEF(THEORY)	CEF(EXP)	CEF(THEORY)	MEF(EXP)	MEF(THEORY)	KEF(EX/TH)	CEF(EX/TH)	MEF(EX/TH)
HOUSING 1	ROTOR 1								
RA=435,000	0.8264E 07	0.6686E 07	0.2099E 05	0.1502E 05	3.619	2.952	1.236	1.398	1.22
RA=325,000	0.3852E 07	0.3967E 07	0.1624E 05	0.1187E 05	19.20	2.318	0.9710	1.369	8.28
RA=150,000	0.5826E 06	0.8296E 06	2863.	5749.	4.778	1.532	0.7023	0.4980	3 11
RA= 75,000	-0.2889E 06	0.2731E 06	1369.	2964.	7.571	1.213	-1.058	0.4620	6.24
RA= 50,000	-0.1894E 06	0.1225E 06	522.1	2238.	6.075	1.430	-1.545	0.2333	4 24
HOUSING 1	ROTOR 2								
RA= 50,000	0.2082E 06	0.9708E 05	1098.	2018.	2.412	1.769	2.145	0.5442	1.36
RA= 75,000	0.3946E 06	0.3827E 05	1451.	2784.	3.071	2.876	10.31	0.5212	1.06
RA=150,000	0.1192E 07	0.8570E 06	4122.	5944.	5.012	0.9988	1.390	0.6934	5 01
RA=335,000	0.4745E 07	0.4145E 07	0.1382E 05	0.1209E 05	9.460	-0.5657	1.145	1.143	-16.7
RA=450,000	0.8973E 07	0.6657E 07	0.2058E 05	0.1461E 05	-2.615	1.794	1.348	1.408	-1.45
HOUSING 1	ROTOR 4								
RA= 50,000	0.5094E 06	0.1421E 06	837.2	1899.	-3.935	1.261	3.585	0.4408	-3 11
RA= 75,000	0.7992E 06	0.3982E 06	1647.	3262.	-4.759	-1.182	2.007	0.5049	4 02
RA=150,000	0.1900E 07	0.1069E 07	4628.	6447	2.362	0.1831	1.778	0.7177	12.9
RA=325,000	0.8013E 07	0.4719E 07	0.2081E 05	0.1423E 05	12.22	0.1999	1.698	1.463	61.1
RA=345,000	0.9892E 07	0.4858E 07	0.2089E 05	0.1522E 05	-7.406	1.683	2.037	1.373	-4.40
HOUSING 1	ROTOR 5								
RA= 50,000	-0.4863E 05	0.9736E 05	755.3	1921.	6.240	1.786	-0.4995	0.3932	3 49
RA= 75,000	-0.4094E 05	0.2257E 06	1585.	3005.	9.222	1.704	-0.1814	0.5275	5 41
RA=150,000	0.8287E 06	0.9184E 06	4749.	6021.	11.84	2.196	0.9023	0.7888	5 39
RA=325,000	0.7241E 07	0.4618E 07	0.1627E 05	0.1372E 05	-1.466	2.105	1.568	1.185	-0.696
RA=380,000	0.9206E 07	0.5666E 07	0.1935E 05	0.1505E 05	-7.613	2.879	1.625	1.286	-2 64
HOUSING 2	ROTOR 1								
RA= 75,000	0.1308E 06	0.2462E 06	3530.	3239.	20.86	-0.6043	0.5313	1.090	-34.5
RA=125,000	0.7659E 06	0.1011E 07	6787.	5834.	29.98	-1.561	0.7577	1.163	-19.2
RA=150,000	0.1386E 07	0.1393E 07	9197.	7421.	24.98	-1.463	0.9949	1.239	-16.8
RA=275,000	0.5912E 07	0.4347E 07	0.2187E 05	0.1265E 05	24.51	-0.1735	1.360	1.729	-141.
RA=330,000	0.8049E 07	0.5942E 07	0.2343E 05	0.1481E 05	36.44	0.3675	1.355	1.583	99.1
HOUSING 2	ROTOR 4								
RA= 75,000	0.1017E 07	0.3823E 06	5586.	4086.	-3.496	-1.197	2.661	1.367	2.92
RA=150,000	0.2089E 07	0.1747E 07	0.1152E 05	8942.	19.79	-2.101	1.196	1.288	-9 42
RA=270,000	0.5061E 07	0.5150E 07	0.2117E 05	0.1516E 05	-3.745	-6.654	0.9828	1.397	0.562
HOUSING 2	ROTOR 5								
RA= 75,000	-0.5772E 05	0.2922E 06	2734.	4034.	16.21	0.8217	-0.1976	0.6779	19.7
RA=125,000	0.2427E 06	0.1137E 07	6638.	7133.	25.60	0.1081	0.2135	0.9307	236.
RA=275,000	0.3842E 07	0.5154E 07	0.2044E 05	0.1463E 05	7.951	0.3100E-01	0.7455	1.397	256.
RA=290,000	0.4905E 07	0.5778E 07	0.1851E 05	0.1457E 05	-5.850	-2.056	0.8490	1.270	2 84
HOUSING 3	ROTOR 1								
RA=106,000	0.6500E 06	0.3577E 06	3732.	3788.	10.53	1.003	1.817	0.9852	10.5
RA=163,000	0.1447E 07	0.1264E 07	6972.	6736.	19.94	0.8037E-01	1.145	1.035	248.
RA=303,000	0.7211E 07	0.4141E 07	0.1827E 05	0.1256E 05	11.81	1.504	1.742	1.455	7 85
RA=355,000	0.9857E 07	0.5503E 07	0.2243E 05	0.1446E 05	4.242	1.740	1.791	1.551	2 43
HOUSING 3	ROTOR 4								
RA=106,000	0.1598E 07	0.5907E 06	2746.	5522.	-0.9733	-0.8495	2.706	0.4974	1 14
RA=164,000	0.2536E 07	0.1487E 07	7136.	8592.	7.962	-0.4882E-01	1.705	0.8305	-163.
RA=288,000	0.7181E 07	0.4469E 07	0.1942E 05	0.1435E 05	9.343	-2.395	1.607	1.354	-3.90
HOUSING 3	ROTOR 5								
RA=106,000	0.7214E 06	0.5841E 06	3819.	5504.	13.70	-1.332	1.235	0.6938	-10.2
RA=155,000	0.1495E 07	0.1250E 07	7248.	7802.	17.72	-0.3380	1.197	0.9290	-52.4
RA=305,000	0.8124E 07	0.4939E 07	0.1984E 05	0.1445E 05	10.18	-0.5865	1.645	1.373	-17.3

Table 2. Measured and finite-length theoretical [4] predictions for effective direct stiffness, damping, and added-mass coefficients.

TAPERED SEAL SHORT SEAL THEORY SEAL 2 (TAPERED)
SI UNITS

	KEF(EXP)	KEF(THEORY)	CEF(EXP)	CEF(THEORY)	MEF(EXP)	MEF(THEORY)	KEF(EX/TH)	CEF(EX/TH)	MEF(EX/TH)
HOUSING 1	ROTOR 1								
RA=435,000	0.8264E 07	0.8717E 07	0.2099E 05	0.1536E 05	3.619	2.642	0.9481	1.366	1.37
RA=325,000	0.3852E 07	0.5118E 07	0.1624E 05	0.1184E 05	19.20	2.835	0.7527	1.371	6.77
RA=150,000	0.5826E 06	0.1018E 07	2863.	4712.	4.778	1.983	0.5722	0.6077	2.41
RA= 75,000	-0.2889E 06	0.3421E 06	1369.	2048.	7.571	1.517	-0.8443	0.6688	4.99
RA= 50,000	-0.1894E 06	0.1671E 06	522.1	1561.	6.075	1.372	-1.133	0.3345	4.42
HOUSING 1	ROTOR 2								
RA= 50,000	0.2082E 06	0.1504E 06	1098.	1405.	2.412	1.568	1.385	0.7815	1.53
RA= 75,000	0.3946E 06	0.3704E 05	1451.	1896.	3.071	3.451	10.65	0.7652	0.889
RA=150,000	0.1192E 07	0.1073E 07	4122.	5025.	5.012	1.015	1.110	0.8203	4.93
RA=335,000	0.4745E 07	0.5392E 07	0.1382E 05	0.1217E 05	9.460	-1.807	0.8801	1.136	-5.23
RA=450,000	0.8973E 07	0.8622E 07	0.2058E 05	0.1505E 05	-2.615	1.941	1.041	1.367	-1.34
HOUSING 1	ROTOR 4								
RA= 50,000	0.5094E 06	0.1748E 06	837.2	1770.	-3.935	0.9202	2.914	0.4729	-4.27
RA= 75,000	0.7992E 06	0.4923E 06	1647.	2856.	-4.759	-2.047	1.623	0.5767	2.32
RA=150,000	0.1900E 07	0.1380E 07	4628.	5658.	2.362	-0.5893	1.377	0.8178	-4.00
RA=325,000	0.8013E 07	0.6040E 07	0.2081E 05	0.1412E 05	12.22	-0.3843E-01	1.327	1.474	-317.
RA=345,000	0.9892E 07	0.6164E 07	0.2089E 05	0.1525E 05	-7.406	2.430	1.605	1.370	-3.04
HOUSING 1	ROTOR 5								
RA= 50,000	-0.4863E 05	0.1329E 06	755.3	1662.	6.240	1.341	-0.3658	0.4544	4.65
RA= 75,000	-0.4094E 05	0.2982E 06	1585.	2382.	9.222	1.310	-0.1373	0.6656	7.04
RA=150,000	0.8287E 06	0.1168E 07	4749.	4974.	11.84	2.115	0.7093	0.9547	5.59
RA=325,000	0.7241E 07	0.5946E 07	0.1627E 05	0.1342E 05	-1.466	2.288	1.218	1.212	-0.640
RA=380,000	0.9206E 07	0.7190E 07	0.1935E 05	0.1485E 05	-7.613	3.883	1.280	1.303	-1.96
HOUSING 2	ROTOR 1								
RA= 75,000	0.1308E 06	0.2959E 06	3530.	2756.	20.86	-1.395	0.4420	1.281	-14.9
RA=125,000	0.7659E 06	0.1269E 07	6787.	5032.	29.98	-2.354	0.6035	1.349	-12.7
RA=150,000	0.1386E 07	0.1761E 07	9197.	6601.	24.98	-2.324	0.7870	1.393	-10.7
RA=275,000	0.5912E 07	0.5530E 07	0.2187E 05	0.1194E 05	24.51	-0.7926	1.069	1.832	-30.9
RA=330,000	0.8049E 07	0.7524E 07	0.2343E 05	0.1410E 05	36.44	0.2502	1.070	1.661	145.
HOUSING 2	ROTOR 4								
RA= 75,000	0.1017E 07	0.4841E 06	5586.	3914.	-3.496	-2.445	2.101	1.427	1.43
RA=150,000	0.2089E 07	0.2225E 07	0.1152E 05	8521.	19.79	-3.000	0.9387	1.352	-6.59
RA=270,000	0.5061E 07	0.6452E 07	0.2117E 05	0.1480E 05	-3.745	-6.984	0.7845	1.431	0.536
HOUSING 2	ROTOR 5								
RA= 75,000	-0.5772E 05	0.3589E 06	2734.	3754.	16.21	0.3352	-0.1608	0.7283	48.3
RA=125,000	0.2427E 06	0.1456E 07	6638.	6588.	25.60	-0.5785	0.1667	1.008	-44.2
RA=275,000	0.3842E 07	0.6487E 07	0.2044E 05	0.1411E 05	7.951	0.6207	0.5923	1.449	12.8
RA=290,000	0.4905E 07	0.7402E 07	0.1851E 05	0.1391E 05	-5.850	-4.937	0.6627	1.330	1.18
HOUSING 3	ROTOR 1								
RA=106,000	0.6500E 06	0.4328E 06	3732.	3055.	10.53	0.5045	1.502	1.221	20.8
RA=163,000	0.1447E 07	0.1595E 07	6972.	5650.	19.94	-0.4782	0.9074	1.234	-41.6
RA=303,000	0.7211E 07	0.5233E 07	0.1827E 05	0.1169E 05	11.81	1.851	1.378	1.563	6.38
RA=355,000	0.9857E 07	0.6956E 07	0.2243E 05	0.1376E 05	4.242	1.876	1.417	1.631	2.26
HOUSING 3	ROTOR 4								
RA=106,000	0.1598E 07	0.7431E 06	2746.	5239.	-0.9733	-1.806	2.150	0.5242	0.539
RA=164,000	0.2536E 07	0.1915E 07	7136.	8069.	7.962	-0.8935	1.324	0.8844	-8.91
RA=288,000	0.7181E 07	0.5657E 07	0.1942E 05	0.1395E 05	9.343	-3.064	1.269	1.392	-3.05
HOUSING 3	ROTOR 5								
RA=106,000	0.7214E 06	0.7264E 06	3819.	5120.	13.70	-2.356	0.9930	0.7458	-5.81
RA=155,000	0.1495E 07	0.1594E 07	7248.	7169.	17.72	-1.083	0.9383	1.011	-16.3
RA=305,000	0.8124E 07	0.6268E 07	0.1984E 05	0.1399E 05	10.18	-1.049	1.296	1.419	-9.71

Table 3. Measured and improved short-seal theoretical [4] predictions for effective direct stiffness, damping, and added-mass coefficients.

TAPERED SEAL THEORY   SEAL 2 (TAPERED)

UNITS ARE N/M

	KEF (EXP)	KEF (THEORY)	KEF (EXP/THE)	CEF (EXP)	CEF (THEORY)	CEF (EXP/THE)
HOUSING 1	ROTOR 1					
RA=435,000	0.8264E 07	0.9511E 07	0.8689	0.2099E 05	0.1919E 05	1.094
RA=325,000	0.3852E 07	0.5255E 07	0.7330	0.1624E 05	0.1501E 05	1.082
RA=150,000	0.5826E 06	0.1241E 07	0.4695	2863.	6561.	0.4364
RA= 75,000	-0.2889E 06	0.1589E 06	-1.818	1369.	4329.	0.3162
RA= 50,000	-0.1894E 06	0.1651E 06	-1.147	522.1	3617.	0.1443
HOUSING 1	ROTOR 2					
RA= 50,000	0.2082E 06	-0.2951E 06	-0.7055	1098.	6076.	0.1807
RA= 75,000	0.3946E 06	-0.5617E 05	-7.025	1451.	6050.	0.2398
RA=150,000	0.1192E 07	0.1133E 07	1.052	4122.	6865.	0.6004
RA=335,000	0.4745E 07	0.5640E 07	0.8413	0.1382E 05	0.1609E 05	0.8589
RA=450,000	0.8973E 07	0.9450E 07	0.9495	0.2058E 05	0.2044E 05	1.007
HOUSING 1	ROTOR 4					
RA= 50,000	0.5094E 06	0.2701E 06	1.886	837.2	1711.	0.4893
RA= 75,000	0.7992E 06	0.4103E 06	1.948	1647.	2632.	0.6258
RA=150,000	0.1900E 07	0.1860E 07	1.022	4628.	5800.	0.7979
RA=325,000	0.8013E 07	0.8986E 07	0.8917	0.2081E 05	0.1371E 05	1.518
RA=345,000	0.9892E 07	0.9419E 07	1.050	0.2089E 05	0.1472E 05	1.419
HOUSING 1	ROTOR 5					
RA= 50,000	-0.4863E 05	0.1695E 06	-0.2869	755.3	1815.	0.4161
RA= 75,000	-0.4094E 05	0.3645E 06	-0.1123	1585.	2821.	0.5619
RA=150,000	0.8287E 06	0.1519E 07	0.5456	4749.	5910.	0.8036
RA=325,000	0.7241E 07	0.7728E 07	0.9370	0.1627E 05	0.1500E 05	1.085
RA=380,000	0.9206E 07	0.9935E 07	0.9266	0.1935E 05	0.1662E 05	1.164
HOUSING 2	ROTOR 1					
RA= 75,000	0.1308E 06	0.5072E 06	0.2579	3530.	3498.	1.009
RA=125,000	0.7659E 06	0.1412E 07	0.5424	6787.	5752.	1.180
RA=150,000	0.1386E 07	0.1952E 07	0.7100	9197.	6879.	1.337
RA=275,000	0.5912E 07	0.6323E 07	0.9350	0.2187E 05	0.1229E 05	1.779
RA=330,000	0.8049E 07	0.8845E 07	0.9100	0.2343E 05	0.1445E 05	1.621
HOUSING 2	ROTOR 4					
RA= 75,000	0.1017E 07	0.6449E 06	1.577	5586.	3331.	1.677
RA=150,000	0.2089E 07	0.2618E 07	0.7979	0.1152E 05	7171.	1.606
RA=270,000	0.5061E 07	0.7640E 07	0.6624	0.2117E 05	0.1287E 05	1.645
HOUSING 2	ROTOR 5					
RA= 75,000	-0.5772E 05	0.6502E 06	-0.8877E-01	2734.	3896.	0.7017
RA=125,000	0.2427E 06	0.1605E 07	0.1512	6638.	6318.	1.051
RA=275,000	0.3842E 07	0.7853E 07	0.4892	0.2044E 05	0.1354E 05	1.510
RA=290,000	0.4905E 07	0.8373E 07	0.5858	0.1851E 05	0.1384E 05	1.337
HOUSING 3	ROTOR 1					
RA=106,000	0.6500E 06	0.7782E 06	0.8353	3732.	4030.	0.9261
RA=163,000	0.1447E 07	0.1925E 07	0.7517	6972.	6152.	1.133
RA=303,000	0.7211E 07	0.6818E 07	1.058	0.1827E 05	0.1238E 05	1.476
RA=355,000	0.9857E 07	0.9160E 07	1.076	0.2243E 05	0.1461E 05	1.535
HOUSING 3	ROTOR 4					
RA=106,000	0.1598E 07	0.1190E 07	1.343	2746.	4370.	0.6284
RA=164,000	0.2536E 07	0.2877E 07	0.8815	7136.	6990.	1.021
RA=288,000	0.7181E 07	0.8448E 07	0.8500	0.1942E 05	0.1325E 05	1.466
HOUSING 3	ROTOR 5					
RA=106,000	0.7214E 06	0.9918E 06	0.7274	3819.	4687.	0.8148
RA=155,000	0.1495E 07	0.2142E 07	0.6979	7248.	6888.	1.052
RA=305,000	0.8124E 07	0.8780E 07	0.9253	0.1984E 05	0.1394E 05	1.423

Table 4. Measured and original short-seal theoretical [2] predictions for effective direct stiffness and damping coefficients (Table 34, ref. [1]).

TAPERED SEAL THEORY SEAL 2 (TAPERED)
UNITS ARE kg

	MEF (EXP)	MEF (THEORY)	MEF (EXP/THE)
HOUSING 1	ROTOR 1		
RA=435,000	3.619	4.952	0.7309
RA=325,000	19.20	7.563	2.539
RA=150,000	4.778	6.709	0.7122
RA= 75,000	7.571	10.77	0.7027
RA= 50,000	6.075	10.18	0.5965
HOUSING 1	ROTOR 2		
RA= 50,000	2.412	25.65	0.9402E-01
RA= 75,000	3.071	17.92	0.1714
RA=150,000	5.012	8.489	0.5903
RA=335,000	9.460	7.808	1.211
RA=450,000	-2.615	6.481	-0.4034
HOUSING 1	ROTOR 4		
RA= 50,000	-3.935	3.522	-1.117
RA= 75,000	-4.759	4.074	-1.168
RA=150,000	2.362	2.275	1.038
RA=325,000	12.22	0.4564	26.76
RA=345,000	-7.406	3.546	-2.088
HOUSING 1	ROTOR 5		
RA= 50,000	6.240	4.852	1.286
RA= 75,000	9.222	4.972	1.855
RA=150,000	11.84	5.480	2.160
RA=325,000	-1.466	4.107	-0.3569
RA=380,000	-7.613	3.668	-2.076
HOUSING 2	ROTOR 1		
RA= 75,000	20.86	3.540	5.892
RA=125,000	29.98	2.428	12.35
RA=150,000	24.98	-0.5142	-48.58
RA=275,000	24.51	1.419	17.27
RA=330,000	36.44	1.333	27.34
HOUSING 2	ROTOR 4		
RA= 75,000	-3.496	1.999	-1.749
RA=150,000	19.79	-0.7368	-26.86
RA=270,000	-3.745	1.129	-3.316
HOUSING 2	ROTOR 5		
RA= 75,000	16.21	2.098	7.726
RA=125,000	25.60	2.913	8.788
RA=275,000	7.951	0.2855	27.85
RA=290,000	-5.850	3.145	-1.860
HOUSING 3	ROTOR 1		
RA=106,000	10.53	3.316	3.176
RA=163,000	19.94	3.103	6.425
RA=303,000	11.81	2.147	5.499
RA=355,000	4.242	2.908	1.459
HOUSING 3	ROTOR 4		
RA=106,000	-0.9733	1.198	-0.8123
RA=164,000	7.962	0.5052	15.76
RA=288,000	9.343	1.526	6.122
HOUSING 3	ROTOR 5		
RA=106,000	13.70	2.238	6.121
RA=155,000	17.72	1.270	13.95
RA=305,000	10.18	1.262	8.070

Table 5. Measured and original short-seal theoretical [2] predictions for effective added-mass coefficients (Table 40, ref. [2]).

The results of these error calculations are presented in Table 6 below.

	EK	EC	EM
Finite	1.618	2.14	111.7
Improved Short	.042	1.27	78.8
Original Short	.049	2.96	4.45

Table 6. Least square error calculations for the first two data sets of Tables 2 through 5.

Obviously, minimum values of error are desirable. For prediction of effective stiffness and damping coefficients, the improved short-seal solution is seen to be the best. However, the original short-seal solutions is much better for calculating the equivalent added-mass coefficient. More specifically, measured added-mass coefficients are much larger than predicted by either the finite-length or the improved short-seal solution.

APPENDIX A

FINITE-LENGTH SOLUTIONS FOR THE ROTORDYNAMIC COEFFICIENTS OF CONVERGENT-TAPERED ANNULAR SEALS

D. W. Childs
Mechanical Engineering Department
Texas A&M University
College Station, Texas 77843

ABSTRACT

A combined analytical-computational method is developed to calculate the pressure field and dynamic coefficients for convergent-tapered high-pressure annular seals which are typical of neck-ring and interstage seals employed in multistage centrifugal pumps. Completely developed turbulent flow is assumed in both the circumferential and axial directions, and is modeled by Hirs' bulk-flow turbulent-lubrication equations. Linear zeroth and first-order perturbation equations are developed for the momentum equations and continuity equation. The development of the circumferential velocity field is defined from the zeroth-order circumferential-momentum equation, and the nominal pressure-leakage relationship results from the zeroth-order axial-momentum equation.

The first-order perturbation yields three partial differential equations which are reduced to three ordinary, complex, differential equations in the axial coordinate z. These linear equations are integrated to satisfy the boundary conditions, and define the pressure distribution due to seal motion. Integration of the pressure distribution defines the reaction force developed by the seal and the corresponding rotordynamic coefficients. The solution does not employ linearization with respect to the magnitude of the taper angle or the degree of swirl. Finite-length solutions are compared to "short-seal" solutions.

NOMENCLATURE

a_i:	Dimensionless coefficients defined in Appendix C.
b:	Dimensionless coefficient defined in Eq.(9).
$\tilde{c}$, $\tilde{C}$:	Dimensionless damping coefficients defined by Eq.(34).
C_d:	Seal discharge coefficient defined by Eq.(15).
f(z):	Dimensionless clearance function defined by Eq.(2).
$h(z) = H/C$:	Dimensionless clearance function.
$h_1 = H_1/C$:	First-order perturbation clearance function defined by Eq.(4) and (18).
$\tilde{k}$, $\tilde{K}$	Dimensionless seal stiffness coefficients defined by Eq.(34).
$\tilde{m}$, $\tilde{M}$	Dimensionless mass coefficients defined by Eq.(34).
$mo = -0.25$, $no = 0.079$:	Coefficients for Hirs' turbulent lubrication equations.
p:	Fluid pressure (F/L^2).
p_o:	Zeroth-order perturbation pressure introduced in Eq.(4), (F/L^2).
p_1:	First-order perturbation pressure introduced in Eq.(4), (F/L^2).
$\tilde{p}_1$:	Dimensionless perturbation pressure defined in Eq.(8).
q:	Taper-angle parameter defined in Eq.(3).
t:	Independent variable time (T).
$u_Z = U_Z/R\omega$, $u_\theta = U_\theta/R\omega$:	Dimensionless axial and circumferential velocity components.
$u_{\theta 0}$, $u_{\theta 1}$:	Zeroth and first-order perturbations in u_θ.
u_{Z0}, u_{Z1}:	Zeroth and first-order perturbations in u_Z.
v:	Dimensionless swirl variable introduced in Eq.(7), and defined by Eq.(11).
v_o:	Initial (z=0) swirl.
$z = Z/L$	Dimensionless axial coordinate.

$\overline{C}$:	Nominal seal radial clearance, (L).
C_0, C_1:	Entrance and exit clearances, respectively, (L).
$H(z,\theta,t)$:	Clearance function, introduced in Eq.(4), and defined in Eq.(17), (L).
$H_o(z)$:	Centered-clearance function defined by Eq.(2), (L).
$H_1(\theta,t)$:	First-order perturbation in H, introduced in Eq.(4), (L).
L:	Seal length (L).
P_s:	Seal supply pressure (F/L^2).
ΔP:	Nominal pressure-drop across seal (F/L^2).
R:	Seal radius (L).
$R_c = \rho(R\omega)H/\mu$:	Circumferential Reynolds number.
$R_a = 2\rho VH/\mu$:	Axial Reynolds number.
$R_{co} = \rho(R\omega)\overline{C}f/\mu$:	Centered-position, circumferential Reynolds number.
$R_{ao} = 2\rho\overline{V}\overline{C}/\mu$:	Centered-position, axial Reynolds number.
$T = L/\overline{V}$:	Transit time for a fluid element to traverse the seal.
$U = R\omega$:	Seal tangential velocity.
U_Z, U_θ:	Axial and tangential fluid velocity components (L/T).
V(z):	Centered-position axial fluid velocity (L/T).
$\overline{V}$:	Centered-position average fluid velocity (L/T).
X, Y:	Radial seal displacements (L).
Z, $R\theta$:	Spatial coordinates illustrated in Figure 2.
α:	Seal taper angle illustrated in Figure 2.
ε:	Seal eccentricity ratio introduced in Eq.(4).
ξ	Inlet pressure-loss coefficient.

λ:	Dimensionless friction-factor defined in Eq.(9).
$\sigma = \lambda L/C$	
$\tau = t/T$:	Dimensionless time.
ω:	Shaft angular velocity (T^{-1}).
Ω:	Shaft precessional velocity (T^{-1}), introduced in Eq.(23).

INTRODUCTION

In a series of publications, Black et al. [1-3] have explained the considerable influence of seal forces on the rotordynamic behavior of pumps. Figure 1 illustrates the two seal types which have the potential for developing significant rotor forces. The neck or wear-ring seals are provided to reduce the back leakage flow along the front surface of the impeller face, while the interstage seal reduces the leakage from an impeller inlet back along the shaft to the backside of the preceding impeller. Pump seals are geometrically similar to plain journal bearings, but have clearance-to-radius ratios on the order of 0.005, as compared to 0.001 for bearings. Because of the clearances, and normally-experienced pressure differentials, fully-developed turbulent flow normally exists in pump seals.

As related to rotordynamics, analysis of seals has the objective of defining the reaction forces acting on the rotor as a consequence of shaft motion. For small motion about a centered position, the relation between the reaction-force components and shaft motion may be expressed by

$$-\begin{Bmatrix} F_X \\ F_Y \end{Bmatrix} = \begin{bmatrix} K & k \\ -k & K \end{bmatrix} \begin{Bmatrix} X \\ Y \end{Bmatrix} + \begin{bmatrix} C & c \\ -c & C \end{bmatrix} \begin{Bmatrix} \dot{X} \\ \dot{Y} \end{Bmatrix} + \begin{bmatrix} M & m \\ -m & M \end{bmatrix} \begin{Bmatrix} \ddot{X} \\ \ddot{Y} \end{Bmatrix} \tag{1}$$

Unlike hydrodynamic bearings, seals develop significant direct stiffness in the centered, zero-eccentricity position due to the distribution of the axial pressure drop between (a) inlet losses and (b) an axial pressure gradient due to friction losses. Further, experiments [2] have shown that the above relationship holds for fairly large eccentricities on the order of 0.5; i.e., the dynamic coefficients (K,k,C,c,M,m) tend to be relatively insensitive to changes in static eccentricity ratios.

Prior analysis to define seal rotordynamic coefficients has involved the following developments:

(a) Black and Jenssen [2], [3] used a bulk-flow analysis, with the circumferential bulk-flow velocity assumed to be fully-developed shear flow at $\frac{R\omega}{2}$. In these analyses, the axial-momentum equation incorporates Yamada's [4] friction-factor results for flow through rotating concentric cylinders, with the friction factor defined by average circumferential and axial Reynolds numbers. In analogy to "short-bearing" solutions, a short-seal solution is developed, which accounts for the circumferential flow due to shear, but neglects that due to pressure. The short-seal solution provides a definition for the dynamic coefficients of Eq. (1).

(b) In an appendix to [1], an approximate finite-length solution is developed, and correction factors are developed as a function of L/D ratios for the short-seal dynamic-coefficient solutions.

(c) In [3], Black and Jenssen define the friction factor as a function of the local axial and radial Reynolds numbers, i.e., the local clearance.

(d) Allaire et al. [5] used Black's model to numerically calculate dynamic coefficients at large eccentricity ratios. Further, while Black and Jenssen define seal coefficients in a coordinate frame that rotates at half the shaft angular velocity, and employ a coordinate transformation to achieve stationary-reference results, Allaire et al. perform all calculations in a stationary reference frame.

(e) Black et al. [6] combined prior seal-analysis governing equations with equations previously derived for the analysis of "Journal-bearings with high axial-flow in the turbulent regime," to examine the development of circumferential flow in a centered seal as a function of axial seal position. They demonstrate that the circumferential velocity starts from an arbitrary initial velocity and asymptotically approaches $\frac{R\omega}{2}$ as it proceeds axially along the seal. Stated differently, they account for the influence of inlet swirl. Predictions of the stiffness cross-coupling coefficient are generally reduced if the development of circumferential flow is accounted for in seal analysis. This analysis does not include the dependence of the friction-factor on local Reynolds numbers, i.e., local clearance introduced in [3].

(f) Childs [7] performed an analysis of straight turbulent seals for small motion about a centered position based on Hirs' turbulent lubrication equations [8]. The short-seal analysis was employed under less restrictive assumptions than those previously employed to derive seal dynamic coefficients. A single derivation, from one set of governing equations, yields results which include all previous "short-seal" solution developments.

(g) Childs [9] completed a finite-length solution for straight turbulent seals using the Hirs-based model of [7].

(h) Fleming [10] analyzed straight seals with one-step and convergent tapered seals; concluding that optimally tapered seals can develop considerably higher direct stiffnesses than straight seals. Fleming's analysis yields only the direct stiffness term, and does not include the effect of swirl; hence, his results are not adequate for a rotordynamic analysis of pump response or stability. Childs [11] performed short-seal analysis of convergent-tapered seals based on Hirs lubrication equations which defines all of the required dynamic coefficients of Eq. (1).

The present analysis yields finite-length solutions for convergent-tapered seal geometries. The model is analyzed using the method of reference [9]; however, unlike preceding analyses, linearization assumptions are not required with respect to the magnitude of either the taper angle or swirl.

Seal Geometry

Figure 2 illustrates the seal geometry. The clearance at the centered position is defined by

$$H_0 = (\overline{C} + \frac{\alpha L}{2}) - \alpha Z = \overline{C}[1 + q(1 - 2z)] = f\overline{C} \tag{2}$$

where α is the seal taper angle, and

$$\overline{C} = (C_0 + C_1)/2, \quad z = Z/L, \quad q = \frac{\alpha L}{2\overline{C}} = \frac{C_0 - C_1}{C_0 + C_1} \tag{3}$$

The ratio of entrance to exit clearances is

$$\frac{C_0}{C_1} = \frac{1 + q}{1 - q}$$

The clearance ratio C_0/C_1 is the following tabular function of q

C_0/C_1	∞	7	3	2	1.67	1.285
q	1	0.75	0.5	0.333	0.25	0.125

where q = 1 corresponds to a zero-clearance exit. Given that Fleming's optimum stiffness choices for C_0/C_1 are between 1.8 and 2.2, maximum values for q to be expected in practice would be less than 0.4.

Simplified Perturbation Equations

Hirs' governing equations are provided in Appendix A, and are thoroughly discussed in reference[8]. These bulk-flow equations define the axial and circumferential velocity components (u_Z, u_θ) and the pressure, p, as a function of the spatial variables (R_θ,Z) and time, t. The equations are expanded in the perturbation variables

$$u_Z = u_{Z0} + \varepsilon u_{Z1} \quad , \quad H = H_0 + \varepsilon H_1 \tag{4}$$

$$u_\theta = u_{\theta 0} + \varepsilon u_{\theta 1} \quad , \quad p = p_0 + \varepsilon p_1$$

where $\varepsilon = e/\overline{C}$ is the eccentricity ratio, to yield the perturbation equations of Appendix B.

These perturbation equations may be markedly simplified by carrying out the following steps:

(a) Introduce the following nondimensional variables

$$z = Z/L, \quad \tau = t/T \tag{5}$$

where T is the fluid transit time defined by

$$T = L/\overline{V} \tag{6}$$

(b) Introduce the swirl variable v defined by

$$u_{\theta 0} = \tfrac{1}{2} + v \tag{7}$$

(c) Introduce the nondimensional perturbation pressure

$$\tilde{p}_1 = p_1/\rho\overline{V}^2 \tag{8}$$

where $\overline{V}$ is the average fluid velocity.

(d) Identify the friction-factor coefficient

$$\sigma = \frac{\lambda L}{\overline{C}} , \quad \lambda = noR_{ao}^{mo}\left[1 + \frac{1}{4b^2}\right]^{\frac{1 + mo}{2}} , \; b = \frac{\overline{V}}{R\omega} \tag{9}$$

The parameter λ can be factored out of the terms noA_i occurring in Appendix B. This factoring step yields the a_i coefficients of the following equations, as defined in Appendix C.

Following these steps, the governing equations become

Zeroth-Order Equations

(a) Axial-Momentum Equation

$$\frac{dp_o}{dz} = -\frac{\rho\overline{V}^2}{f^3}(\sigma a_o + 2q) \tag{10}$$

(b) Circumferential-Momentum Equation

$$\frac{dv}{dz} + \frac{\sigma}{2f}a_1 = 0 \tag{11}$$

First-Order Equations

The first-order equations of Appendix B are additionally simplified by substitution from Eqs(10) and (11) to yield

(a) Axial-Momentum Equation

$$-\frac{\partial\tilde{p}_1}{\partial z} = -(1 - mo)\sigma a_o\frac{h_1}{f^4} + \left[\sigma a_o + (1 + mo)\frac{\sigma a_3}{2} + \frac{2q}{\sigma}\right]\frac{u_{Z1}}{bf^2}$$
$$+(1 + mo)\sigma a_2\frac{u_{\theta 1}}{2f^3} + \frac{1}{b}\left[\frac{\partial u_{Z1}}{\partial\tau} + \omega T(\tfrac{1}{2} + v)\frac{\partial u_{Z1}}{\partial\theta} + \frac{1}{f}\frac{\partial u_{Z1}}{\partial z}\right] \tag{12}$$

(b) Circumferential-Momentum Equation

$$-\left(\frac{L}{R}\right)\frac{\partial\tilde{p}_1}{\partial\theta} = -(1 - mo)\sigma a_1\frac{h_1}{2bf^3} + [2\sigma a_o + (1 + mo)\sigma a_4]\frac{u_{\theta 1}}{2bf^2} \tag{13}$$
$$+\left[\frac{(1 + mo)\sigma a_2}{2f^2} - \frac{\sigma a_1}{2b^2}\right]u_{Z1} + \frac{1}{b}\left[\frac{\partial u_{\theta 1}}{\partial\tau} + \omega T(\tfrac{1}{2} + v)\frac{\partial u_{\theta 1}}{\partial\theta} + \frac{1}{f}\frac{\partial u_{\theta 1}}{\partial z}\right]$$

(c) Continuity Equation

$$\frac{\partial u_{Z1}}{\partial z} + \left(\frac{L}{R}\right)\frac{\partial u_{\theta 1}}{\partial\theta} - \frac{2q}{f}u_{Z1} = \frac{-b}{f}\left[\frac{2qh_1}{f^2} + \omega T(\tfrac{1}{2} + v)\frac{\partial h_1}{\partial\theta} + \frac{\partial h_1}{\partial\tau}\right] \tag{14}$$

In contrast to earlier developments [7,9,11], q and v are not treated as small parameters in obtaining these equations.

Zeroth-Order Perturbation Solutions

The zeroth-order continuity equation has the solution H_0U_{Z0} = constant, and the centered-position axial-velocity distribution is accordingly defined in terms of the volumetric flowrate Q and cross-sectional area by

$$V(z) = Q/2\pi RH_0 = Q/2\pi R\bar{C}f = \bar{V}/f$$

where $\bar{V}$ is the average or mid-seal velocity. Hence,

$$u_{Z0} = V(z)/R\omega = b/f$$

Eq.(11), the circumferential-momentum equation which defines v, is non-linear, but may be integrated numerically without difficulty. Alternately, linearization of Eq.(11) in terms of q and v yields a reasonable approximation of the nonlinear solution, [11]. The nonlinear numerical solution is used in the present study.

Linearization of the zeroth-order axial-momentum Eq.(10) in q and v is helpful in providing an initial estimate for leakage, and yields the following steady-state relationship

$$\Delta P = C_d \frac{\rho\bar{V}^2}{2} \cong \frac{\rho\bar{V}^2}{2} \left\{ \frac{1+\xi}{(1+q)^2} + \frac{4q + 2\sigma[1 - \beta(1 + mo)q^2]}{(1 - q^2)^2} \right\} \tag{15}$$

where

$$\beta = 1/(1 + 4b^2),$$

and ξ is the entry-loss coefficient. The term

$$\Delta P_0 = \frac{\rho\bar{V}^2}{2} \frac{(1+\xi)}{(1+q)^2} \tag{16}$$

accounts for the total pressure drop at the inlet, while the remaining terms account for the pressure drop due to wall friction and Bernoulli effects. For a specified ΔP, Eq.(15) may be solved iteratively for the average velocity $\bar{V}$ and associated leakage. The exact solution is obtained by iteratively solving the coupled differential Eqs.(10) and (11).

First-Order Equation Solutions

The preceding equations define $p_1(z,\theta,\tau)$, $u_{Z1}(z,\theta,\tau)$, and $u_{\theta 1}(z,\theta,\tau)$ resulting from the seal clearance function $h_1(\theta,\tau)$. The clearance H is defined in terms of the components of the seal-journal displacement vector (X,Y) by

$$H = H_0 - X\cos\theta - Y\sin\theta \tag{17}$$

Hence, by comparison to Eq. (4)

$$\varepsilon h_1 = -x\cos\theta - y\sin\theta \tag{18}$$

where

$$x = X/\overline{C}\ ,\ y = Y/\overline{C}$$

Note that h_1 is not a function of z, and its time dependency arises from the displacement variables x(t), y(t).

Solutions for the equations cited above must satisfy the circumferential continuity conditions

$$u_{Z1}(z,\tau,\theta) = u_{Z1}(z,\tau,\theta+2\pi)$$

$$u_{\theta 1}(z,\tau,\theta) = u_{\theta 1}(z,\tau,\theta+2\pi)$$

$$\tilde{p}_1(z,\tau,\theta) = \tilde{p}_1(z,\tau,\theta+2\pi)$$

To satisfy these conditions, the following solution format is assumed

$$\begin{aligned} u_{Z1}(z,\tau,\theta) &= u_{Z1C}(z,\tau)\cos\theta + u_{Z1S}(z,\tau)\sin\theta \\ u_{\theta 1}(z,\tau,\theta) &= u_{\theta 1C}(z,\tau)\cos\theta + u_{\theta 1S}(z,\tau)\sin\theta \qquad (19) \\ \tilde{p}_1(z,\tau,\theta) &= \tilde{p}_{1C}(z,\tau)\cos\theta + \tilde{p}_{1S}(z,\tau)\sin\theta \end{aligned}$$

Substituting from Eqs. (18) and (19) into Eq. (12) eliminates θ as an independent variable, and yields two real equations. By introducing the complex variables

REFERENCES

1. H. F. Black, "Effects of Hydraulic Forces in Annular Pressure Seals on the Vibrations of Centrifugal Pump Rotors," J. M.Eng. Sci., Vol. 11, No. 2, pp. 206-213, 1969.

2. H. F. Black and D. N. Jenssen, "Dynamic Hybrid Properties of Annular Pressure Seals," Proc. J. Mech. Engr., Vol. 184, pp. 92-100, 1970.

3. H. F. Black and D. N. Jenssen, "Effects of High-Pressure Ring Seals on Pump Rotor Vibrations," ASME Paper No. 71-WA/FF-38, 1971.

4. Y. Yamada, "Resistance of Flow through an Annulus with an Inner Rotating Cylinder," Bull. J.S.M.E., Vol. 5, No. 18, pp. 302-310, 1962.

5. P. E. Allaire, E. J. Gunter, C. P. Lee, and L. E. Barrett, "The Dynamic Analysis of the Space Shuttle Main Engine High Pressure Fuel Turbopump Final Report, Part II, Load Capacity and Hybrid Coefficients for Turbulent Interstage Seals," University of Virginia Report UVA/528140/ME76/103, September 1976.

6. H. F. Black, P. E. Allaire, and L. E. Barrett, "The Effect of Inlet Flow Swirl on the Dynamic Coefficients of High-Pressure Annular Clearance Seals," Ninth International Conference in Fluid Sealing, BHRA Fluid Engineering, Leeuwenhorst, The Netherlands, 1981.

7. D. Childs, "Dynamic Analysis of Turbulent Annular Seals based on Hirs' Lubrication Equation," ASME Paper No. 82-Lub-41, ASME/ASLE 1982 Lubrication Conference, accepted for publication ASME Trans., J. of Lubrication Technology.

8. G. G. Hirs, "A Bulk-Flow Theory for Turbulence in Lubricant Films, "ASME J. of Lub. Tech., pp. 137-146, April 1973.

9. D. Childs, "Finite-Length Solutions for Rotor-Dynamic Coefficients of Turbulent Annular Seals," ASME Paper No. 82-Lub-42, ASME/ASLE 1982 Lubrication Conference, accepted for publication, ASME Trans., J. of Lubrication Technology.

10. D. P. Fleming, "High Stiffness Seals for Rotor Critical Speed Control," ASME Paper 77-DET-10, Design Engineering Technical Conference, Chicago, IL., 26-30 September 1977.

11. D. W. Childs, "Convergent-Tapered Annular Seals: Analysis for Rotordynamic Coefficients," Fluid/Structure Interaction in Turbomachinery, pp. 35-44, ASME 1981.

Appendix C: Definition of a_i

$$2a_oB = G_1 + G_2$$

$$a_1B = (v + ½)G_1 + (v - ½)G_2$$

$$a_2B = \left(\frac{f}{b}\right)^2[(v + ½)G_3 + (v - ½)G_4]$$

$$a_3B = G_3 + G_4$$

$$a_4B = \left(\frac{f}{b}\right)^2[(v + ½)^2G_3 + (v - ½)^2G_4]$$

where

$$B = \left(1 + \frac{1}{4b^2}\right)^{\frac{1+mo}{2}}$$

$$G_1 = \left\{1 + [f(v + ½)/b]^2\right\}^{\frac{1+mo}{2}}$$

$$G_2 = \left\{1 + [f(v - ½)/b]^2\right\}^{\frac{1+mo}{2}}$$

$$G_3 = \left\{1 + [f(v + ½)/b]^2\right\}^{\frac{mo-1}{2}}$$

$$G_4 = \left\{1 + [f(v - ½)/b]^2\right\}^{\frac{mo-1}{2}}$$

where

$$A_2 = u_{\theta 0}\,(u_{\theta 0}^2 + u_{Z0}^2)^{\frac{mo-1}{2}} + (u_{\theta 0} - 1)[(u_{\theta 0} - 1)^2 + u_{Z0}^2]^{\frac{mo-1}{2}}$$

$$A_3 = u_{Z0}^2 \left\{ (u_{\theta 0}^2 + u_{Z0}^2)^{\frac{mo-1}{2}} + [(u_{\theta 0} - 1)^2 + u_{Z0}^2]^{\frac{mo-1}{2}} \right\}$$

(b) Circumferential-Momentum Equation

$$\frac{-H_0^2}{\mu U} \frac{1}{R} \frac{\partial p_1}{\partial \theta} = \frac{no}{2} R_{CO}^{1+mo} (1 + mo) A_1 \left(\frac{H_1}{H_0}\right)$$

$$+ \frac{no}{2} R_{CO}^{1+mo} [A_0 + (1 + mo)A_4] u_{\theta 1}$$

$$+ \frac{no}{2} R_{CO}^{1+mo} (1 + mo) A_2 u_{Z0} u_{Z1}$$

$$+ R_{CO} H_0 \left\{ \frac{1}{U} \frac{\partial u_{\theta 1}}{\partial t} + \frac{u_{\theta 0}}{R} \frac{\partial u_{\theta 1}}{\partial \theta} + u_{Z0} \frac{\partial u_{\theta 1}}{\partial Z} + \left[2\left(\frac{H_1}{H_0}\right) u_{Z0} + u_{Z1} \right] \frac{\partial u_{\theta 0}}{\partial Z} \right\}$$

where

$$A_4 = u_{\theta 0}^2 (u_{\theta 0}^2 + u_{Z0}^2)^{\frac{mo-1}{2}} + (u_{\theta 0} - 1)^2 [(u_{\theta 0} - 1)^2 + u_{Z0}^2]^{\frac{mo-1}{2}}$$

(c) Continuity Equation

$$H_1 \frac{\partial u_{Z0}}{\partial Z} + \frac{\partial}{\partial Z}(H_0 u_{Z1}) + \frac{u_{\theta 0}}{R} \frac{\partial H_1}{\partial \theta} + \frac{H_0}{R} \frac{\partial u_{\theta 1}}{\partial \theta} + \frac{1}{R\omega} \frac{\partial H_1}{\partial t} = 0$$

Appendix B: Tapered Seal Perturbation Equations

Substitution of the perturbation variables of Eq.(2) into the equations of Appendix A yields the following perturbation equations:

Zeroth-Order Equations

(a) Axial-Momentum Equation

$$\frac{-H_0^2}{\mu U}\frac{dp_0}{dZ} = \frac{no}{2} R_{CO}^{1+mo} u_{ZO} A_0 + R_{CO} H_0 u_{ZO} \frac{du_{ZO}}{dZ}$$

$$A_0 = \left(u_{\theta 0}^2 + u_{ZO}^2\right)^{\frac{1+mo}{2}} + \left[(u_{\theta 0} - 1)^2 + u_{ZO}^2\right]^{\frac{1+mo}{2}}$$

(b) Circumferential-Momentum Equation

$$H_0 u_{ZO} \frac{du_{\theta 0}}{dZ} + \frac{no}{2} R_{CO}^{mo} A_1 = 0$$

$$A_1 = u_{\theta 0}\left[u_{\theta 0}^2 + u_{ZO}^2\right]^{\frac{1+mo}{2}} + (u_{\theta 0} - 1)\left[(u_{\theta 0} - 1)^2 + u_{ZO}^2\right]^{\frac{1+mo}{2}}$$

(c) Continuity Equation

$$u_{ZO} = b/f$$

First-Order Equations

(a) Axial-Momentum Equations

$$\frac{-H_0^2}{\mu U}\frac{\partial p_1}{\partial Z} = \frac{2H_0H_1}{\mu U}\frac{\partial p_0}{\partial Z} + \frac{no}{2} R_{CO}^{1+mo}(1 + mo)A_0 u_{ZO}\left(\frac{H_1}{H_0}\right)$$

$$+ \frac{no}{2} R_{CO}^{1+mo}\left[A_0 + (1 + mo)A_3\right]u_{Z1}$$

$$+ \frac{no}{2} R_{CO}^{1+mo}(1 + mo)A_2 u_{ZO} u_{\theta 1}$$

$$+ H_0 R_{CO}\left\{\frac{1}{U}\frac{\partial u_{Z1}}{\partial t} + \frac{u_{\theta 0}}{R}\frac{\partial u_{Z1}}{\partial \theta} + u_{ZO}\frac{\partial u_{Z1}}{\partial Z} + \left[2\left(\frac{H_1}{H_0}\right)u_{ZO} + u_{Z1}\right]\frac{\partial u_{ZO}}{\partial Z}\right\}$$

ORIGINAL PAGE IS
OF POOR QUALITY

Appendix A: Hirs' Turbulent Lubrication Equations

Hirs' turbulent lubrication equations [8] define a bulk-flow theory which does not explicitly make any assumptions concerning either (a) local flow velocity due to turbulence, or (b) the shape of average flow-velocity profiles. Only the bulk-flow relative to a surface or wall and the corresponding shear stress at that surface or wall are considered or correlated. Hirs' axial and circumferential momentum equations can be stated, respectively, as

$$\frac{-H^2}{\mu U}\frac{\partial p}{\partial Z} = \frac{no}{2} R_C^{1+mo}\left\{u_Z(u_\theta^2 + u_Z^2)^{\frac{1+mo}{2}} + u_Z[(u_\theta - 1)^2 + u_Z^2]^{\frac{1+mo}{2}}\right\}$$
$$+ R_C\left\{\frac{H}{U}\frac{\partial u_Z}{\partial t} + \frac{Hu_\theta}{R}\frac{\partial u_Z}{\partial \theta} + Hu_Z\frac{\partial u_Z}{\partial Z}\right\} \qquad (A.1)$$

$$\frac{-H^2}{\mu U}\frac{1}{R}\frac{\partial p}{\partial \theta} = \frac{no}{2} R_C^{1+mo}\left\{u_\theta(u_\theta^2 + u_Z^2)^{\frac{1+mo}{2}} + (u_\theta - 1)[(u_\theta - 1)^2 + u_Z^2]^{\frac{1+mo}{2}}\right\}$$
$$+ R_C\left\{\frac{H}{U}\frac{\partial u_\theta}{\partial t} + \frac{Hu_\theta}{R}\frac{\partial u_\theta}{\partial \theta} + Hu_Z\frac{\partial u_\theta}{\partial Z}\right\} \qquad (A.2)$$

with the bulk-flow continuity equation

$$\frac{\partial(Hu_Z)}{\partial Z} + \frac{1}{R}\frac{\partial}{\partial \theta}(Hu_\theta) + \frac{1}{R\omega}\frac{\partial H}{\partial t} = 0 \qquad (A.3)$$

where $R_o = Cr_o$ is the amplitude of seal motion. The components are expressed as a function of ΩT, because for a given seal geometry (L,R,C) and set of operating conditions ($\Delta P,\omega$), the excitation frequency ΩT is the only independent variable. Stated-differently, Eq. (33) provides a frequency-response solution for the reaction force components.

To calculate seal coefficients, a comparable statement of reaction-force components is developed from the following nondimensional statement of Eq. (1)

$$- \frac{\lambda}{\pi R \Delta P} \begin{Bmatrix} F_X \\ F_Y \end{Bmatrix} = \begin{bmatrix} \tilde{K} & \tilde{k} \\ -\tilde{k} & \tilde{K} \end{bmatrix} \begin{Bmatrix} X \\ Y \end{Bmatrix} + T \begin{bmatrix} \tilde{C} & \tilde{c} \\ -\tilde{c} & \tilde{C} \end{bmatrix} \begin{Bmatrix} \dot{X} \\ \dot{Y} \end{Bmatrix} + T^2 \begin{bmatrix} \tilde{M} & \tilde{m} \\ -\tilde{m} & \tilde{M} \end{bmatrix} \begin{Bmatrix} \ddot{X} \\ \ddot{Y} \end{Bmatrix} \quad (34)$$

Substitution from Eq. (32) yields

$$\frac{\lambda F_r(\Omega T)}{\pi R \Delta P R_o} = \tilde{K} + \tilde{c}(\Omega T) - \tilde{M}(\Omega T)^2 = \frac{2\sigma}{C_d} \int_0^1 f_{3C}(z)dz$$

$$\frac{\lambda F_\theta(\Omega T)}{\pi R \Delta P R_o} = \tilde{k} - \tilde{C}(\Omega T) - \tilde{m}(\Omega T)^2 = \frac{-2\sigma}{C_d} \int_0^1 f_{3S}(z)dz \quad (35)$$

Hence, the dynamic seal coefficients ($\tilde{K},\tilde{k},\tilde{C},\tilde{c},\tilde{M},\tilde{m}$) may be obtained by comparing the solution obtained by Eq. (33) with Eq. (35). More specifically, they are obtained by a least-square curve-fit of the solutions stated on the right-hand side of Eq. (35)

Dynamic Coefficient Definitions

Having obtained the pressure-field solution of Eq. (30), solution for the dynamic coefficients will now be undertaken. The reaction-force components acting on the rotor due to shaft motion are defined by

$$F_X(t) = -\varepsilon RL \int_0^1 \int_0^{2\pi} p_1 \cos\theta d\theta dz = -\varepsilon RL\rho\overline{V}^2 \int_0^1 \int_0^{2\pi} \tilde{p}_1 \cos\theta d\theta dz$$

$$F_Y(t) = -\varepsilon RL \int_0^1 \int_0^{2\pi} p_1 \sin\theta d\theta dz = -\varepsilon RL\rho\overline{V}^2 \int_0^1 \int_0^{2\pi} \tilde{p}_1 \sin\theta d\theta dz$$

From the last of Eq. (18), these integrals further reduce to

$$F_X(t) = -\varepsilon RL\pi\rho\overline{V}^2 \int_0^1 \tilde{p}_{1C} dz \; ; \; F_Y(t) = -\varepsilon RL\pi\rho\overline{V}^2 \int_c^1 p_{1S} dz \qquad (31)$$

The motion defined by Eq. (22) is orbital at the precessional frequency Ω and radius R_o. This statement may be confirmed by comparing the last of Eq. (19) with Eq. (22) to obtain

$$X = \overline{C}r_o \cos\Omega t \quad , \quad Y = \overline{C}r_o \sin\Omega t \qquad (32)$$

Definition of the reaction forces is simplified by performing the integration at a time when the rotating displacement vector is pointing along the X axis, i.e., when $\Omega t = 0$. Eq. (24) shows that $\underline{p}_1$ and $\overline{p}_1$ coincide for this time and location. Hence, Eq. (31) yields the following component force definitions parallel and normal to the displacement vector

$$F_r(\Omega T) = -\, r_o(\pi RL\rho\overline{V}^2) \int_0^1 f_{3C}(z) dz$$

$$F_\theta(\Omega T) = -\, r_o(\pi RL\rho\overline{V}^2) \int_0^1 f_{3S}(z) dz$$

A useful nondimensional version of these equations is

$$\frac{\lambda F_r(\Omega T)}{\pi R \Delta P R_o} = \frac{-2\sigma}{C_d} \int_0^1 f_{3C}(z) dz$$

$$\frac{\lambda F_\theta(\Omega T)}{\pi R \Delta P R_o} = \frac{-2\sigma}{C_d} \int_0^1 F_{3S}(z) dz \qquad (33)$$

$$\underline{u}_{Z1} = u_{Z1C} + j\, u_{Z1S}$$

ORIGINAL PAGE IS
OF POOR QUALITY

$$\underline{u}_{\theta 1} = u_{\theta 1C} + j\, u_{\theta 1S}$$

$$\tilde{\underline{p}}_1 = \tilde{p}_{1C} + j\, \tilde{p}_{1S} \qquad (20)$$

$$\frac{\underline{h}_1}{\varepsilon} = \frac{x}{\varepsilon} + j\, \frac{y}{\varepsilon}\,,$$

these two equations may be combined to obtain

$$\frac{\partial \underline{u}_{Z1}}{\partial z} - jf\omega T(\tfrac{1}{2} + v)\underline{u}_{Z1} + f\,\frac{\partial \underline{u}_{Z1}}{\partial \tau} + \frac{\sigma}{f}\left[a_o + (1 + mo)\,\frac{a_3}{2} + \frac{2q}{\sigma}\right]\underline{u}_{Z1}$$
$$+ \frac{b\sigma}{2f^2}\,(1 + mo)a_2\,\underline{u}_{\theta 1} + bf\,\frac{\partial \underline{p}_1}{\partial z} = \frac{-b\sigma}{f^3}\,(1 - mo)a_o\left(\frac{\underline{h}_1}{\varepsilon}\right) \qquad (21)$$

A similar operation on Eqs.(13) and (14) yields

$$\frac{\partial \underline{u}_{\theta 1}}{\partial z} - jf\omega T(\tfrac{1}{2} + v)\underline{u}_{\theta 1} + f\,\frac{\partial \underline{u}_{\theta 1}}{\partial \tau} + \frac{\sigma}{f}\left[a_o + (1 + mo)\,\frac{a_4}{2}\right]\underline{u}_{\theta 1} \qquad (22)$$
$$+ \frac{b\sigma}{2f^2}\left[(1 + mo)a_2 - f^2\frac{a_1}{b^2}\right]\underline{u}_{Z1} - jfb\left(\frac{L}{R}\right)\underline{p}_1 = \frac{-\sigma}{2f^2}(1 - mo)a_1\left(\frac{\underline{h}_1}{\varepsilon}\right)$$

$$\frac{\partial \underline{u}_{Z1}}{\partial z} - j\left(\frac{L}{R}\right)\underline{u}_{\theta 1} - \frac{2q}{f}\,\underline{u}_{Z1} = \frac{b}{f}\left[\frac{\partial}{\partial \tau}\left(\frac{\underline{h}_1}{\varepsilon}\right) - j\omega T(\tfrac{1}{2} + v)\left(\frac{\underline{h}_1}{\varepsilon}\right) + \frac{2q}{f^2}\left(\frac{\underline{h}_1}{\varepsilon}\right)\right]$$

The time-dependency in these equations is eliminated by assuming a harmonic seal motion of the form

$$\underline{h}_1 = \frac{R_o}{C}\,e^{j\Omega t} = r_o e^{j\Omega T\tau} \qquad (23)$$

where r_o is a <u>real</u> constant. The associated harmonic solution can then be stated

$$\underline{u}_{Z1}(z,\tau) = \bar{u}_{Z1}\,(z)\;e^{j\Omega T\tau}$$

$$\underline{u}_{\theta 1}(z,\tau) = \bar{u}_{\theta 1}\,(z)\;e^{j\Omega T\tau} \qquad (24)$$

$$\underline{p}_1(z,\tau) = \bar{p}_1(z)\;e^{j\Omega T\tau}$$

Substitution from Eqs. (23) and (24) into Eqs. (19) and (20) yields

$$\frac{d}{dz}\begin{Bmatrix}\bar{u}_{Z1}\\ \bar{u}_{\theta 1}\\ \bar{p}_1\end{Bmatrix} + [A]\begin{Bmatrix}\bar{u}_{Z1}\\ \bar{u}_{\theta 1}\\ \bar{p}_1\end{Bmatrix} = \left(\frac{r_o}{\varepsilon}\right)\begin{Bmatrix}g_1\\ g_2\\ g_3\end{Bmatrix} \tag{25}$$

where

$$[A] = \begin{bmatrix} \frac{-2q}{f} & -j\left(\frac{L}{R}\right) & 0 \\ \frac{b\sigma}{2f^2}\left[(1+mo)a_2 - f^2\frac{a_1}{b^2}\right] & \frac{\sigma}{2f}\left[2a_o + a_4(1+mo)\right] + jf\Gamma T & -jfb\left(\frac{L}{R}\right) \\ \frac{\sigma}{bf^2}\left[a_o + \frac{a_3}{2}(1+mo) + 4q\right] + j\frac{\Gamma T}{b} & \frac{\sigma(1+mo)}{2f^3}a_2 + j\frac{\omega T}{f} & 0 \end{bmatrix} \tag{26}$$

$$\begin{Bmatrix}g_1\\ g_2\\ g_3\end{Bmatrix} = \begin{Bmatrix} b\left(\frac{2q}{f^3} + j\frac{\Gamma T}{f}\right) \\ -(1-mo)\sigma a_1/2f^2 \\ -[2q + (1-mo)\sigma a_o]/f^4 + j\Gamma T/f^2 \end{Bmatrix}$$

where

$$\Gamma = \Omega - \omega(\tfrac{1}{2} + v)$$

The following three boundary conditions are specified for the solution of Eq. (25):

(a) The exit perturbation pressure is zero, i.e.,

$$\bar{p}_1(L) = 0 \tag{27}$$

(b) The entrance circumferential velocity perturbation is zero, i.e.,

$$u_{\theta 1}(0) = 0 \tag{28}$$

(c) The pressure loss at the seal entrance is defined by

$$P_S - p(0,\theta,\tau) = \frac{\rho}{2}U_Z^2(0,\theta,\tau)(1+\xi)$$

This equation yields the following perturbation-variable boundary conditior

$$\bar{p}_1(0) = -(1+\xi)\,\bar{u}_{Z10}/b(1+q) \tag{29}$$

Solution of the differential Eqs. (25) in terms of the boundary conditions is relatively straightforward, yielding a solution for the velocity and pressure fields of the form

$$\begin{Bmatrix} \bar{u}_{Z1} \\ \bar{u}_{\theta 1} \\ \bar{p}_1 \end{Bmatrix} = \left(\frac{r_o}{\varepsilon}\right) \begin{Bmatrix} f_{1C}(z) + j\ f_{1S}(z) \\ f_{2C}(z) + j\ f_{2S}(z) \\ f_{3C}(z) + j\ f_{3S}(z) \end{Bmatrix} \tag{30}$$